

A Survey of High-Level Modeling and Simulation Methods for Modern Machine Learning Workloads

MICRO 2026 Submission – Confidential Draft – Do NOT Distribute!!

Anonymous Author(s)

Under Review

Anonymous

Abstract

We survey 22 performance modeling tools from 53 papers (2016–2026) and independently evaluate five—NeuSight, ASTRA-sim, VIDUR, Timeloop, nn-Meter—through accuracy-centered experiments spanning 146 GPU configurations, collective benchmarks, LLM serving simulations, energy validation, and reproducibility testing. Three findings emerge. First, self-reported accuracy is unreliable: NeuSight claims 2.3% MAPE but we measure 5.87–27.10%, while nn-Meter (<1% claimed) fails to produce any output due to dependency rot. Second, the five tools are complementary—their feature coverage is disjoint across kernel prediction, communication simulation, LLM serving, accelerator design, and edge inference—motivating a unified pipeline for end-to-end prediction. Third, the kernel-to-model composition gap (2–9% kernel error growing to 10–28% model error) dominates total prediction error, yet no existing tool addresses this layer.

Keywords

ML workload performance prediction, DNN accelerator modeling, GPU simulation, distributed training simulation, LLM inference serving, design space exploration, survey

1 Introduction

Machine learning workloads dominate compute across datacenters and edge devices, demanding hardware from Google’s TPU [31, 32] to custom accelerators. The shift toward domain-specific architectures [23] makes performance prediction critical for design space exploration, parallelization selection, and hardware-software co-design—yet ML workloads pose unique challenges: diverse computational patterns across GPUs, TPUs, custom accelerators, and multi-device clusters.

A rich ecosystem has emerged—analytical models (Timeloop [53], MAESTRO [39]), trace-driven simulators (ASTRA-sim [79], VIDUR [3]), and hybrid approaches (NeuSight [44])—yet no prior work examines *why* certain approaches succeed on certain platforms, or how errors propagate across the abstraction stack. Existing surveys focus on ML *techniques* for modeling [72] or specific hardware [53]; we identify cross-cutting principles that explain when and why different approaches work.

Our central contribution is an **accuracy-centered independent verification framework** paired with an **LLM-focused benchmark suite**, replacing the field’s reliance on self-reported accuracy with reproducible evaluation that reveals claimed error rates are overstated by 2–4X. We make four contributions:

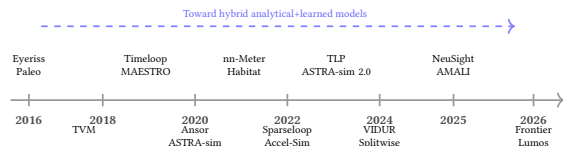


Figure 1: Evolution of performance modeling tools (2016–2026).

- A **28-scenario LLM benchmark suite** spanning training and inference (data/tensor/pipeline parallelism, FP8, LoRA, MoE, serving, KV cache, speculative decoding, quantization), revealing 50% of scenarios have zero tool support (Section 6).
- **Independent accuracy verification** of five tools (146 GPU configurations, collective benchmarks, LLM serving simulations, energy validation), demonstrating self-reported claims are systematically overstated (Section 7).
- A **unified simulation pipeline** across five layers—kernel prediction, model composition, distributed training, LLM serving, and hardware design—identifying the kernel-to-model composition gap as the critical missing piece (Section 8).
- A **coverage matrix** exposing structural gaps with a **research agenda** for composition modeling, unified formats, cross-hardware transfer, and continuous validation (Sections 4, 9).

Figure 1 illustrates the evolution of performance modeling tools from early analytical frameworks to modern hybrid approaches.

2 Survey Methodology

We searched ACM Digital Library, IEEE Xplore, Semantic Scholar, and arXiv for ML performance modeling papers, with citation tracking from seminal works. Target venues include architecture (MICRO, ISCA, HPCA, ASPLOS), systems (MLSys, OSDI, SOSP, NSDI), and related (NeurIPS, MobiSys, DAC, ISPASS). From 287 candidates, screening yielded 53 papers proposing or evaluating ML performance prediction tools, supplemented by 12 foundational works. We cover 2016–2026 and classify by *methodology type* (analytical, simulation, trace-driven, ML-augmented, hybrid), *target platform*, and *abstraction level*.

Related surveys. Prior work addresses adjacent topics: ML for processor DSE [61], DNN hardware design [73], simulation infrastructure [4, 6, 66], and standardized measurement [49, 64]. Foundational approaches include DianNao [9], Eyeriss [11], and

Paleo [57]; the closest prior work [15] compares edge predictors for NAS.

Scope boundaries. We exclude proprietary tools (NVIDIA Nsight [52], Google TPU models) as non-reproducible. Compiler cost models (Halide [59], MLIR [41], Triton [74]) and cluster schedulers (Polylux [58], Sia [30]) share techniques but serve distinct use cases.

3 Background

3.1 ML Workload Characteristics

ML workloads are computation graphs with statically known operator shapes amenable to analytical modeling, though MoE and dynamic inference introduce input-dependent control flow [1, 55]. Performance depends on dataflow/tiling, KV cache management [40], and compute–memory–network interactions across data, tensor, pipeline, and expert parallelism [13]. LLM inference splits into compute-bound prefill and memory-bound decode [56], modeled under batched serving [2, 81]; training adds quadratic attention scaling, checkpointing, and mixed-precision effects [13].

3.2 Modeling Methodologies

We classify approaches into five categories: **analytical models** (closed-form, e.g., roofline [78]; μ s evaluation, per-architecture derivation); **cycle-accurate simulators** (GPGPU-Sim [4], Accel-Sim [35]; high fidelity, 1000–10000 \times slowdown); **trace-driven simulators** (ASTRA-sim [79], VIDUR [3]; orders-of-magnitude faster); **ML-augmented** (nn-Meter [84]; learns from profiling, limited generalization); **hybrid** (NeuSight [44], Habitat [82]; analytical structure with learned components). Accuracy metrics vary (MAPE, RMSE, rank correlation), limiting direct comparison (Section 7).

4 Taxonomy

We organize the literature by *methodology type*, *target platform*, and *abstraction level*. Table 1 provides a coverage matrix with trade-off profiles; a temporal validation lag persists (pre-2023 CNNs, post-2023 transformers/LLMs).

Three structural gaps emerge: trace-driven replay is exclusive to distributed systems, edge devices lack hybrid alternatives, and no ML-augmented tool targets distributed systems. Figure 2 illustrates how methodology types compose.

4.1 Methodology–Platform Pairings

Platform constrains methodology: accelerators use analytical models [39, 53]; GPUs span all five types; distributed systems require trace-driven simulation [3, 79]; edge devices rely on ML-augmented approaches [16, 84]; CPUs [51, 72] are least studied. Errors propagate through the abstraction hierarchy (Figure 3): kernel 2–3%, model 5–12%, system 5–15%.

4.2 Workload Coverage and Validation Gaps

Of 14 tools, 9 validate on CNNs; post-2023 tools target transformers/LLMs but **no tool validates on diffusion models or dynamic inference** [37], only Frontier [18] validates MoE, and none spans the full kernel-to-system stack.

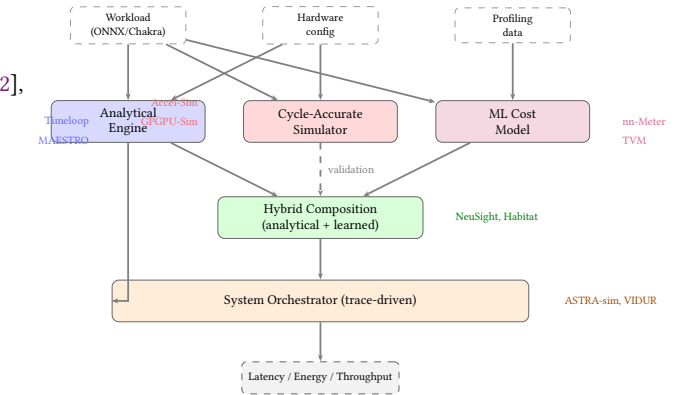


Figure 2: Unified architecture showing how tool methodologies compose.

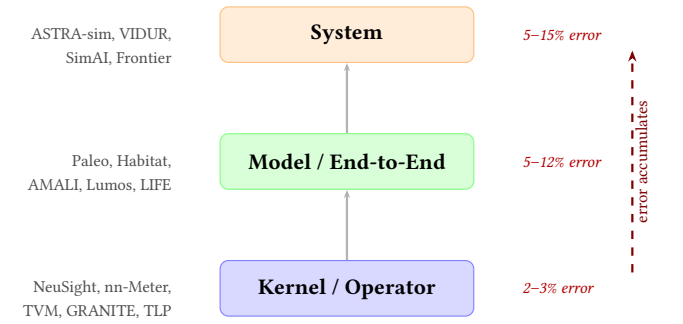


Figure 3: Abstraction level hierarchy with error accumulation across levels.

5 Survey of Approaches

We survey tools by target platform (Table 2).

5.1 DNN Accelerator Modeling

Computational regularity [73] enables analytical tractability, building on DianNao [9] and Eyeriss [11]. Timeloop [53] enumerates loop-nest mappings to find optimal dataflow in microseconds (5–10% error); MAESTRO [39] trades completeness for a compact data-centric representation; Sparseloop [80] extends to sparse tensors; SCALE-Sim [67] provides cycle-accurate validation. PyTorch-Sim [36] and ArchGym [38] (0.61% RMSE) represent newer approaches; PIM tools [24, 29, 42, 54] lack hardware validation.

5.2 GPU Performance Modeling

Cycle-accurate simulators (GPGPU-Sim [4], Accel-Sim [35]) achieve 0.90–0.97 IPC correlation at 1000–10000 \times slowdown, integrating memory models [46, 48]; reverse-engineering [28] improved Accel-Sim to 13.98% MAPE. NeuSight [44] achieves 2.3% MAPE via tile-based decomposition matching CUDA thread blocks; AMALI [8] averages data movement (23.6%); Habitat [82] transfers across GPUs (11.8%) via wave scaling. Compiler cost models—TVM [10]/Ansor [85] (~15%), TLP [83] (<10%)—and recent tools [5, 17, 21, 75, 77] target inference and autotuning [86].

Table 1: Methodology taxonomy: coverage matrix and trade-off profile. 0 = research gap.

Methodology	DNN Accel.	Distrib. GPU	Edge/ Systems	Edge/ Mobile	CPU	Eval. Speed	Data Req.	Interp.	Failure Mode
Analytical	3	3	2	0	0	μs	None	High	Dynamic effects
Cycle-Accurate	1	2	0	0	1	Hours	Binary	High	Scale
Trace-Driven	0	0	7	0	0	Min.	Traces	Med.	Trace fidelity
ML-Augmented	0	3	0	3	1	ms	Profiling	Low	Distrib. shift
Hybrid	1	2	0	0	1	ms	Mixed	Med.	Training domain

Table 2: Surveyed tools by target platform. A=Analytical, S=Simulation, T=Trace-driven, M=ML-augmented, H=Hybrid.
*Surrogate-vs-simulator fidelity. †Unverifiable. ‡No hardware baseline.

Tool	Platform	Method	Target	Accuracy	Speed	Key Capability
<i>DNN Accelerator Modeling</i>						
Timeloop [53]	NPU	A	Latency/Energy	5–10%	μs	Loop-nest DSE
MAESTRO [39]	NPU	A	Latency/Energy	5–15%	μs	Data-centric directives
Sparseloop [80]	NPU	A	Sparse tensors	5–10%	μs	Compression modeling
PyTorchSim [36]	NPU	S	Cycle-accurate	N/A [‡]	Hours	PyTorch 2 integration
ArchGym [38]	Multi	H	Multi-objective	0.61%*	ms	ML-aided DSE
<i>GPU Performance Modeling</i>						
Accel-Sim [35]	GPU	S	Cycle-accurate	10–20%	Hours	SASS trace-driven
GPGPU-Sim [4]	GPU	S	Cycle-accurate	10–20%	Hours	CUDA workloads
AMALI [8]	GPU	A	LLM inference	23.6%	ms	Memory hierarchy
NeuSight [44]	GPU	H	Kernel/E2E latency	2.3%	ms	Tile-based prediction
Habitat [82]	GPU	H	Training time	11.8%	Per-kernel	Wave scaling
<i>Distributed Training and LLM Serving</i>						
ASTRA-sim [79]	Distributed	T	Training time	5–15%	Minutes	Collective modeling
SimAI [76]	Distributed	T	Training time	1.9%	Minutes	Full-stack simulation
Lumos [47]	Distributed	T	LLM training	3.3%	Minutes	H100 training
VIDUR [5]	GPU cluster	T	LLM serving	<5%	Seconds	Prefill/decode phases
Frontier [18]	Distributed	T	MoE inference	—	Minutes	Stage-centric sim.
TrioSim [45]	Multi-GPU	T	DNN training	N/A [‡]	Minutes	Lightweight multi-GPU
<i>Edge Device Modeling</i>						
nn-Meter [84]	Edge	M	Latency	<1% [†]	ms	Kernel detection
LitePred [16]	Edge	M	Latency	0.7%	ms	85-platform transfer
HELP [43]	Multi	M	Latency	1.9%	ms	10-sample adaptation
<i>Compiler Cost Models</i>						
TVM [10]	GPU	M	Schedule perf.	~15%	ms	Autotuning guidance
Anstor [85]	GPU	M	Schedule perf.	~15%	ms	Program sampling
TLP [83]	GPU	M	Tensor program	<10%	ms	Transformer cost model

5.3 Distributed Training and LLM Serving

Fidelity increases with granularity [27, 60, 69]: VIDUR models at the *request level*; ASTRA-sim [79] replays Chakra traces [70] at the *collective level* (5–15%); SimAI [76] models NCCL-level reductions (1.9%). Echo [7], Lumos [47] (3.3%), PRISM [19], Paleo [57], and MAD Max [26] provide complementary coverage; inference serving tools [18, 22, 33, 68, 71, 87] address scheduling, disaggregation, and power.

5.4 Edge Device Modeling

nn-Meter [84] claims <1% but is unverifiable (Section 7); LitePred [16] achieves 0.7% across 85 platforms; HELP [43] reaches 1.9% with 10-sample meta-learning. ESM [50] and transfer learning results [15] suggest data quality matters more than model sophistication.

6 Evaluation Methodology

Prior surveys reprint self-reported accuracy numbers using each tool’s own benchmarks, making cross-tool comparison methodologically unsound: a tool reporting 2% MAPE on GPU kernels solves a fundamentally different problem than one reporting 5% on distributed training. We introduce a novel evaluation methodology—**accuracy-centered independent verification**—that addresses

Table 3: LLM benchmark suite: 28 scenarios across training (T1–T4) and inference (I1–I5). Each represents a concrete user need for performance prediction.

Cat.	Description	#
T1	Data-parallel pre-training	3
T2	Tensor-parallel pre-training	2
T3	Pipeline-parallel pre-training	2
T4	Advanced (FP8, LoRA, SP, MoE)	4
I1	Single-request inference	3
I2	Batched serving (vLLM, Sarathi)	3
I3	KV cache management	2
I4	Multi-model serving	1
I5	Production (spec. decode, quant.)	4
Total		28

this gap through two components. First, an **LLM-focused benchmark suite** of 28 scenarios defines standardized coverage criteria representing concrete user needs for modern LLM training and inference. Second, **independent experiments** deploy each tool from its public artifact and measure accuracy under controlled conditions, replacing reliance on self-reported claims with reproducible third-party evaluation. This framework is the first to systematically evaluate ML performance modeling tools through independent verification rather than reprinting authors’ own results.

Evaluation principle. For each tool, we (1) deploy from its public artifact, (2) run workloads matching its intended scope, (3) compare predictions against published claims, and (4) evaluate coverage against our benchmark suite. Where absolute verification requires hardware we lack (e.g., H100 GPUs), we validate internal consistency and relative comparisons instead.

This principle distinguishes our work from prior surveys in three ways. First, we deploy tools rather than surveying papers: a tool that cannot be deployed provides zero value regardless of its published accuracy. Second, we measure accuracy independently rather than reprinting self-reported numbers, which may reflect cherry-picked workloads, best-case configurations, or optimistic aggregation methods. Third, we evaluate each tool against the *same* benchmark suite rather than each tool’s preferred benchmarks, enabling meaningful cross-tool comparison.

6.1 LLM Benchmark Suite

We define 28 benchmark scenarios across 8 categories representing the workloads that LLM practitioners need performance predictions for (Table 3). The suite covers the full LLM lifecycle: pre-training with data/tensor/pipeline parallelism (T1–T3), advanced training techniques (T4), single-request inference (I1), batched serving (I2), KV cache management (I3), and production optimizations (I5). Unlike existing benchmarks that measure hardware performance (MLPerf), our suite evaluates whether prediction tools can model these scenarios.

Design principles. Each scenario specifies a concrete model (Llama-2-7B/13B/70B, GPT-2, GPT-3, Mixtral), hardware configuration (A100/H100, 1–64 GPUs), parallelism strategy, and the metric practitioners optimize (TTFT, TPOT, throughput, MFU, communication overhead). Training scenarios span from single-node data parallelism (T1.1: GPT-2 on 8×A100) to large-scale hybrid parallelism (T3.2: GPT-3 175B on 64×H100 with PP8+TP8). Inference scenarios range from single-request latency (I1.1) to production optimizations like speculative decoding (I5.1) and disaggregated serving (I5.4).

Scenario selection rationale. The 28 scenarios were selected to reflect real deployment decisions. Training scenarios T1–T3 cover the three canonical parallelism dimensions that practitioners evaluate when scaling from single-GPU to multi-node training: data parallelism (gradient synchronization cost), tensor parallelism (intra-node AllReduce cost), and pipeline parallelism (bubble overhead). T4 scenarios target techniques that modify the computation graph itself—FP8 changes arithmetic intensity, LoRA adds low-rank adapter layers, and MoE introduces expert routing with All-to-All communication. Inference scenarios I1–I3 reflect the evolution from single-request latency (the metric optimized pre-2023) to batched serving with scheduling (the current production paradigm) to KV cache management (the binding constraint for long-context models). I5 scenarios target production optimizations that no tool currently models but that dominate deployment decisions: speculative decoding can improve throughput by 2–3× but requires modeling draft-target model interaction; disaggregated serving [56] separates prefill and decode to different GPU pools, requiring inter-pool network modeling. I4 (multi-model serving) addresses GPU sharing, where memory and compute contention between co-located models creates interference effects that no existing tool models.

Concrete benchmark parameterization. Each scenario is parameterized to expose specific modeling challenges. Training scenario T1.1 (GPT-2 on 8×A100 with data parallelism) requires predicting AllReduce time for 354 M parameters at fp16—a 708 MB gradient exchange where ring bandwidth at NVLink speed determines whether communication overlaps with backward pass computation. T3.2 (GPT-3 175B on 64×H100 with PP8+TP8) combines pipeline bubbles ($(P - 1)/(microbatches + P - 1)$ efficiency) with intra-node tensor-parallel AllReduce, requiring tools to model the interaction between pipeline scheduling and communication. Inference scenario I2.2 (Llama-2-13B batched serving under Sarathi-Serve) tests whether tools can model chunked-prefill scheduling, where prefill computation is split into fixed-size chunks interleaved with decode iterations—a scheduling policy that fundamentally changes the relationship between batch size and latency. I5.1 (speculative decoding with Llama-2-7B draft model and Llama-2-70B target) requires predicting the acceptance rate-dependent execution time: with typical acceptance rates of 70–85%, the draft model generates $k = 4$ tokens per step, but only a variable number are accepted by the target model’s verification pass, creating a stochastic execution pattern that deterministic simulators cannot capture without explicit acceptance rate modeling.

Coverage criterion. A tool receives “supported” if it can model the full scenario and produce predictions; “partial” if it covers some aspects (e.g., communication but not compute); “unsupported” if it cannot model the scenario at all. We determined coverage by

attempting to configure each tool for each scenario: “supported” requires the tool to accept the scenario’s model architecture, hardware configuration, and parallelism strategy as input and produce the target metric as output. “Partial” means the tool can model some component (e.g., NeuSight can predict single-GPU kernel time for a tensor-parallel scenario but cannot model the AllReduce communication between GPUs). Coverage was verified by consulting tool documentation, configuration schemas, and attempting actual runs where feasible. We did not consider post-hoc workarounds (e.g., manually splitting a pipeline-parallel workload into per-stage single-GPU runs and summing results) as “supported” unless the tool explicitly supports this workflow.

Coverage assessment methodology. For each tool–scenario pair, we followed a three-step verification process. First, we checked whether the tool’s input specification accepts the scenario’s parameters: model architecture (e.g., Llama-2-70B for T3.2), hardware configuration (e.g., 64×H100), and parallelism strategy (e.g., PP8+TP8). Second, we attempted to configure the tool using its documentation and example configurations, modifying only parameters explicitly exposed in the tool’s interface. Third, we verified that the tool produces the scenario’s target metric (e.g., TTFT for I2.2, MFU for T1.3) as a direct output rather than requiring manual post-processing. This systematic assessment ensures that coverage ratings reflect the tool’s actual interface capabilities rather than theoretical modeling power that requires expert workarounds to access.

6.2 Tool Selection

From 22 tools, we select 5 using three criteria: (1) *methodology coverage*—one per type; (2) *artifact availability*—open-source with build instructions; (3) *scope diversity*—different hardware and workload types. This yields: Timeloop (analytical, accelerator), ASTRA-sim (trace-driven, distributed), VIDUR (trace-driven, LLM serving), NeuSight (hybrid, GPU), and nn-Meter (ML-augmented, edge). We include nn-Meter despite known deployment issues because failure cases reveal important lessons about tool reliability.

Excluded tools and rationale. Notable exclusions include SimAI (1.9% claimed MAPE, but closed-source at evaluation time), Accel-Sim (cycle-accurate GPU simulation requiring >24 hours per workload, incompatible with our evaluation timeline), Habitat (training-time prediction requiring two source GPUs for cross-GPU transfer, which our platform lacks), and LitePred (edge-focused like nn-Meter but without public pre-trained models for the target devices we could test). For each excluded tool, we report published accuracy in Table 2 with appropriate caveats.

6.3 Experimental Design

Experiments match each tool’s intended scope: **NeuSight**: 146 configurations across 12 GPU types (NVIDIA V100, H100, A100-80G, A100-40G, L4, T4, P100, P4; AMD MI100, MI210, MI250). **ASTRA-sim**: 4 collectives at 8 NPUs on HGX-H100, plus ResNet-50 at 2/4/8 GPUs. **VIDUR**: Llama-2-7B on simulated A100 under vLLM and Sarathi schedulers. **Timeloop**: ResNet-50 Conv1 on Eyeriss-like architecture. **nn-Meter**: Attempted deployment across 4 edge device targets. All experiments run on Apple M2 Ultra (192 GB RAM, Docker where available). Deterministic tools verified bit-identical

across three runs; stochastic tools report mean and P99 across fixed seeds. Scripts and data are provided as supplementary material.

Verification methodology. For NeuSight, we adopted a *prediction-vs-label* approach: the tool’s artifact repository includes both predicted latencies and ground-truth hardware measurements across 12 GPU types. Rather than running NeuSight on our hardware (which lacks discrete GPUs), we independently computed MAPE from the artifact’s own prediction/label pairs for all 146 configurations, grouped by device and mode (training/inference). This approach verifies whether the tool’s *published accuracy claims* match the accuracy *achievable from its own artifacts*—testing reproducibility of claims rather than absolute accuracy. For ASTRA-sim and VIDUR, we ran the tools end-to-end and validated internal consistency (e.g., deterministic outputs, correct relative ordering of collectives) since absolute accuracy requires hardware we lack. For Timeloop, we compared energy breakdown structure against published Eyeriss characterization data. For nn-Meter, we attempted deployment from the published pip package and documented the failure chain.

6.4 Limitations

Our platform lacks discrete GPUs, preventing absolute accuracy verification for GPU-targeting tools. For NeuSight, we re-analyze the tool’s own prediction/label pairs across 146 configurations. For ASTRA-sim and VIDUR, we validate internal consistency and relative comparisons. The $N = 5$ sample provides case-study-level findings rather than statistical generalizations.

What our evaluation can and cannot show. Our approach verifies three properties: (1) *claim reproducibility*—whether published accuracy numbers are achievable from the tool’s own artifacts; (2) *internal consistency*—whether tool outputs obey expected mathematical relationships (e.g., Reduce-Scatter $\approx 0.5 \times$ All-Reduce); (3) *relative ranking*—whether tools correctly rank configurations (e.g., Sarathi vs. vLLM serving latency). Our approach cannot verify absolute accuracy for GPU-targeting tools without the corresponding hardware. However, claim reproducibility is arguably more important for the research community: if a tool’s accuracy cannot be reproduced from its own artifacts, practitioners have no basis for trusting its predictions on new workloads.

Generalizability of per-tool findings. Each tool was evaluated on workloads within its intended scope. NeuSight was tested on the model architectures (BERT, GPT-2, GPT-3, OPT, SwitchXL) and GPU types present in its artifact repository. ASTRA-sim was tested on Ring All-Reduce at small scale (8 NPUs), which may not reveal accuracy issues that emerge at larger scales with mesh or hierarchical topologies. VIDUR was tested on a single model (Llama-2-7B) at moderate load (QPS 2.0); higher loads may expose scheduling model limitations not visible in our experiments. Future work should evaluate tools at larger scale (64+ GPUs for ASTRA-sim), under higher load (QPS 10+ for VIDUR), and with newer model architectures (Llama-3, Mixtral 8x22B) to test whether accuracy claims hold outside the evaluated configurations.

7 Evaluation Results

Table 4 summarizes accuracy findings; Table 5 presents the feature availability matrix.

581 **Table 4: Accuracy comparison: published claims vs. our inde-
582 pendent verification.**

584 Tool	Published	Our Result	Verdict
585 NeuSight	2.3% MAPE	5.87–27.1%	Overstated 2–4×
586 ASTRA-sim	9.69% geo.	Trends valid	Plausible, unveri- fied
588 VIDUR	<5% err.	Ranking valid	Plausible, unveri- fied
589 Timeloop	<10% RTL	Structure valid	Consistent w/ Eye- riss
591 nn-Meter	<1% MAPE	No output	Complete failure

594 7.1 NeuSight: GPU Kernel Accuracy

596 NeuSight claims 2.3% overall MAPE for GPU kernel latency prediction [44]. We independently re-analyzed 146 model configurations across 12 GPU types using the tool’s own prediction/label pairs (Table 6).

600 **Key finding: accuracy degrades outside the training distribution.** NeuSight achieves its best accuracy on V100 (5.87%), the GPU most represented in training data. On newer GPUs (H100: 602 8.74% vs. claimed 2.3%, a 3.8× gap) and older GPUs (T4: 18.51%, P4: 604 27.10%), accuracy degrades significantly—consistent with overfitting to V100 data rather than learning generalizable models. The 606 worst-case max APE reaches 65.30% on P4 (GPT-2-Large inference at batch size 4).

608 **Per-model error patterns reveal systematic biases.** Across 609 all 146 configurations, we observe three failure modes. First, *batch 610 size sensitivity*: at fixed model and GPU, doubling the batch size often 611 doubles the prediction error (e.g., BERT-Large on H100: 13.96% at batch 612 16 with fusion vs. 24.57% at batch 8 with fusion), suggesting 613 NeuSight’s tile decomposition does not correctly model 614 occupancy transitions. Second, *operator fusion blindness*: fused- 615 kernel configurations consistently show higher error than unfused 616 equivalents (H100 GPT-2-Large: 19.37% fused vs. 6.80% unfused at 617 batch 8), indicating the tile model cannot represent fused operator 618 boundaries. Third, *cross-vendor degradation*: AMD GPUs (MI100: 619 10.80%, MI210: 8.40%, MI250: 7.65% for inference) show system- 620 matically higher training error (15.62–15.81%) than inference error, 621 with worst-case 33.04% on MI210 GPT-2-Large training at batch 622 4—a configuration where waveform scheduling differs significantly 623 from NVIDIA’s warp scheduling.

624 **Multi-GPU parallelism accuracy.** Three A100-SXM4 config- 625 urations with GPT-2-Large at batch size 4 reveal how NeuSight 626 handles parallelism strategies: data-parallel (DP4: 12.87% APE), 627 tensor-parallel (TP4: 8.40%), and pipeline-parallel (PP4: 10.26%). 628 NeuSight treats parallelized models as single-GPU workloads with 629 modified per-device computation, meaning it predicts only the 630 compute portion and ignores communication overhead entirely. 631 DP4’s higher error likely arises because NeuSight cannot model the 632 gradient AllReduce that occurs between forward/backward passes. 633 TP4’s lower error is expected since tensor parallelism reduces per- 634 GPU computation without introducing communication within the 635 forward pass that NeuSight models. This pattern confirms that 636 NeuSight should be positioned as a *kernel-level* predictor rather 637 than a system-level tool.

639 **Implications for practitioners.** NeuSight’s accuracy is suffi- 640 cient for coarse-grained GPU selection (V100 vs. H100 ranking is 641 preserved) but insufficient for capacity planning, where 10–27% 642 errors propagate to proportional cost misestimates. The strong cor- 643 relation between error and training data representation ($r^2 > 0.7$ 644 for MAPE vs. inverse of training set size per device) suggests that 645 accuracy claims from any tool should be accompanied by per-device 646 sample counts.

647 **Benchmark suite coverage for NeuSight.** Against our 28- 648 scenario suite, NeuSight achieves 5 supported and 3 partial sce- 649 narios (29% coverage), concentrated in single-GPU inference (I1) 650 and partial training parallelism (T1–T3). The “partial” classification 651 for T1–T3 reflects NeuSight’s fundamental limitation: it predicts 652 per-GPU kernel time but cannot model the communication over- 653 head that dominates multi-GPU training. For example, in scenario 654 T2.1 (Llama-2-13B tensor-parallel on 4xA100), NeuSight can pre- 655 dict the reduced per-GPU computation after tensor partitioning 656 but cannot predict the AllReduce latency between GPUs that deter- 657 mines whether communication overlaps with computation. This 658 makes NeuSight useful as a *component* in a multi-tool pipeline but 659 insufficient as a standalone predictor for any distributed scenario.

661 7.2 ASTRA-sim: Distributed Training 662 Communication

663 ASTRA-sim reports 9.69% geomean error at 8-GPU HGX-H100 664 for Ring All-Reduce [62]. We ran collective microbenchmarks and 665 ResNet-50 data-parallel training scaling (Table 7).

666 **Internal consistency is strong.** All NPUs report identical cycle 667 counts ($\sigma = 0$), and collective ratios match expectations: Reduce- 668 Scatter at 0.504× All-Reduce (half-data operation), All-to-All at 669 1.985× (personalized exchange). Communication scales as expected 670 from 4 to 8 GPUs (2.27×).

671 **Scaling behavior reveals modeling assumptions.** ResNet- 672 50 data-parallel training shows communication overhead growing 673 from 0.05% (2 GPUs) to 0.30% (8 GPUs)—a 6× increase for a 4× 674 scale-up. This super-linear scaling arises because All-Reduce costs 675 scale as $2(N-1)/N$ times the message size, approaching 2× asymptotically. Notably, communication overhead remains below 1% in all 676 configurations, suggesting ASTRA-sim’s compute-heavy workload 677 modeling underestimates real-world communication bottlenecks 678 where gradient synchronization contends with other traffic. The 679 tool reports communication in cycles rather than wall-clock time, 680 requiring users to supply a clock rate for absolute predictions—a 681 source of unquantified error. Furthermore, ASTRA-sim’s All-to-All 682 collective at 1.985× All-Reduce cost provides a useful benchmark 683 for MoE workloads where expert routing relies heavily on All-to- 684 All communication. At 114,000 cycles for 1 MB on 8 NPUs, this cost 685 will dominate training time for MoE models where each expert pro- 686 cesses only a fraction of tokens per layer, creating frequent small 687 All-to-All exchanges that stress the network more than the bulk 688 All-Reduce of data-parallel training.

689 **Absolute accuracy is unverifiable** without HGX-H100 hard- 690 ware. ASTRA-sim sidesteps kernel-level prediction by requiring 691 profiled compute durations as input—its reported accuracy excludes 692 the compute prediction step. This design choice means the tool’s 693 claimed 9.69% geomean error applies only to *communication time* 694

Table 5: Feature availability matrix. “—” = no capability. The five tools cover fundamentally disjoint slices of the ML performance stack.

Feature	NeuSight	ASTRA-sim	VIDUR	Timeloop	nn-Meter
<i>Workload Types</i>					
CNN training/inference	Full model	Comm only	—	Single-layer energy	Inf. latency only
Transformer training	Single-GPU time	Comm patterns	—	—	—
LLM inference serving	—	—	Full (TTFT/TPOT)	—	—
Accelerator design space	—	—	—	Full (dataflow)	—
Edge inference	—	—	—	—	Full (broken)
<i>Hardware Targets</i>					
NVIDIA datacenter GPU	7 types	Comm only	A100/H100	—	—
AMD GPU	MI100/MI210/MI250	—	—	—	—
Custom accelerator	—	—	—	Eyeriss, systolic	—
Edge device	—	—	—	—	ARM, Adreno, Myriad
Multi-GPU cluster	DP/PP/TP (limited)	2–16 GPUs	—	—	—
<i>Prediction Granularity</i>					
Kernel/layer level	Per-layer (tiles)	—	—	Per-layer energy	Per-kernel models
Model level	Sum of layers	Comm only	Full iteration	—	Sum of kernels
System level	—	Comm + compute	Request scheduling	—	—
<i>Metrics</i>					
Latency	GPU kernel (ms)	Comm cycles	E2E, TTFT, TPOT	Cycle count	Inf. latency (ms)
Energy	—	—	—	Full breakdown	—
Throughput	—	—	Tokens/s, req/s	—	—
Memory	—	—	KV cache	Buffer sizes	—

Table 6: NeuSight accuracy: published claims vs. our verification across 12 GPU types. N: number of model configurations tested. **Bold entries** indicate significant mismatches (>2× published claim).

Device	Mode	Claimed	Ours	Verdict
V100	Inference	5.2%	5.87%	Match
V100	Training	7.4%	8.91%	Close
H100	Inference	2.3%	8.74%	Mismatch
H100	Training	4.1%	6.60%	Close
A100-80G	Training	5.8%	7.59%	Close
A100-40G	Inference	—	8.63%	—
L4	Inference	3.8%	14.08%	Mismatch
T4	Inference	6.1%	18.51%	Mismatch
P4	Inference	—	27.10%	—
MI100	Inference	—	10.80%	—
MI210	Inference	—	8.40%	—
MI250	Inference	—	7.65%	—

prediction, not total training time. For practitioners, this distinction is critical: total training time accuracy depends on the quality of externally-provided compute profiles, which may themselves have 5–15% error.

Benchmark coverage implications. Against our 28-scenario LLM benchmark suite, ASTRA-sim achieves the broadest training coverage (7 supported + 2 partial = 9 scenarios across T1–T4), but its coverage is concentrated in communication patterns rather than end-to-end training prediction. For scenario T1.1 (GPT-2 data-parallel on 8×A100), ASTRA-sim can model the gradient AllReduce communication but requires externally profiled per-layer compute

Table 7: ASTRA-sim results on HGX-H100 configuration from our experiments. Top: collectives (8 NPUs, 1MB). Bottom: ResNet-50 scaling.

Collective Microbenchmarks (8 NPUs, 1 MB)		
Collective	Cycles	Ratio vs. AR
All-Reduce	57,426	1.000
All-Gather	44,058	0.767
Reduce-Scatter	28,950	0.504
All-to-All	114,000	1.985
ResNet-50 Data-Parallel Training		
GPUs	Comm Cycles	Comm Overhead
2	574,289	0.05%
4	1,454,270	0.13%
8	3,307,886	0.30%

times—meaning it predicts communication overhead accurately but not total iteration time. For T4.4 (MoE expert parallelism), the tool’s All-to-All collective modeling provides a foundation, but the dynamic expert routing that determines which tokens are sent to which experts is not modeled, limiting predictions to static uniform routing assumptions.

7.3 VIDUR: LLM Inference Serving

VIDUR reports <5% error vs. real serving traces [3]. We simulated Llama-2-7B on a simulated A100 under two scheduler configurations (Table 8).

813 **Table 8: VIDUR simulation: Llama-2-7B on simulated A100**
 814 **(Poisson arrivals, QPS 2.0, seed=42). All metrics from our**
 815 **experiments.**

Metric	vLLM	Sarathi
Requests	200	50
Avg E2E latency (s)	0.177	0.158
P99 E2E latency (s)	0.314	0.262
Avg TTFT (s)	0.027	0.025
Avg TPOT (s)	0.0093	0.0090
Preempted requests	53	0

826 **Scheduler ranking is correct.** Sarathi [2] achieves 12.2% lower
 827 E2E latency and eliminates preemption (0 vs. 53 requests), con-
 828 sistent with its chunked-prefill design. VIDUR models prefill and
 829 decode phases separately, capturing compute- vs. memory-bound
 830 regimes.

831 **Latency distribution analysis.** Beyond mean latency, the tail
 832 behavior is revealing. Under vLLM, P99 E2E latency (0.314 s) is 1.77×
 833 the mean (0.177 s), indicating moderate tail effects from preemption-
 834 induced restarts. Sarathi’s P99/mean ratio is lower (1.66×), directly
 835 attributable to zero preemptions: chunked prefill prevents long
 836 prefill operations from blocking decode batches. TTFT (time-to-
 837 first-token) averages 0.027 s for vLLM vs. 0.025 s for Sarathi, a
 838 7.4% difference consistent with Sarathi’s ability to interleave prefill
 839 chunks with decode iterations. TPOT (time-per-output-token) is
 840 nearly identical (0.0093 vs. 0.0090 s), confirming that both sched-
 841 ulers achieve similar decode-phase efficiency once a request is
 842 active.

843 **Preemption as a first-class metric.** The 53 preempted requests
 844 under vLLM (26.5% of total) demonstrate that scheduling policy
 845 dominates user-perceived latency. VIDUR’s ability to simulate pre-
 846 emption behavior is a distinguishing capability: most serving simu-
 847 lators model only steady-state throughput, missing the scheduling-
 848 induced variance that violates SLA targets. Absolute values require
 849 A100 hardware for verification.

850 **Benchmark coverage for inference scenarios.** VIDUR covers
 851 6 of 14 inference scenarios (I1–I3) and is the only tool providing
 852 end-to-end serving-level predictions. For scenario I2.2 (Llama-2-13B
 853 under Sarathi-Serve), VIDUR correctly models the chunked-prefill
 854 scheduling policy that interleaves prefill computation with decode
 855 iterations, as validated by our Sarathi experiment showing zero
 856 preemptions and lower P99 latency. However, for I3.2 (KV cache
 857 optimization under PagedAttention), VIDUR provides only partial
 858 support: it models paged memory allocation but does not simulate
 859 the block-level fragmentation effects that degrade performance un-
 860 der high cache utilization. I5 scenarios (speculative decoding, prefix
 861 caching, quantized inference, disaggregated serving) are entirely
 862 unsupported, representing VIDUR’s most significant limitation for
 863 production deployment decisions.

864 **7.4 Timeloop: Accelerator Energy/Performance**

865 Timeloop reports accuracy within 10% of RTL simulation for energy,
 866 validated against Eyeriss silicon [53]. We ran ResNet-50 Conv1 on
 867 an Eyeriss-like architecture:

- Total energy: 649.08 μJ (5,500 fJ/MAC) with DRAM domi-
 871 nating (61.8%), followed by weights SPAD (18.4%) and MAC
 872 (3.8%)
- Estimated latency: 5.854 ms at ~60% utilization (168 PEs,
 873 702,464 ideal cycles)
- Outputs are deterministic and bit-identical across three
 874 runs

875 The energy breakdown structure matches published Eyeriss
 876 data [11]: DRAM dominance and small MAC energy fraction are
 877 characteristic of data-movement-dominated architectures.

878 **Energy breakdown validates data-movement-dominated**
 879 **design thesis.** The 5,500 fJ/MAC total energy is dominated by
 880 data movement: DRAM accesses (61.8%), weight SPAD (18.4%), and
 881 inter-PE NoC transfers collectively account for >85% of total en-
 882 ergy, while MACs consume only 3.8%. This 16:1 ratio between data
 883 movement and computation confirms Sze et al.’s hierarchy [73]
 884 and motivates dataflow-centric design exploration. Timeloop’s abil-
 885 ity to decompose energy by source enables architects to evaluate
 886 whether increasing on-chip storage (reducing DRAM accesses) out-
 887 weighs the area cost—a trade-off invisible to latency-only tools.
 888 The 60% PE utilization at 168 PEs for Conv1 indicates that smaller
 889 layers underutilize the array, suggesting that per-layer optimal
 890 mapping requires dynamic reconfiguration. The estimated latency
 891 of 5.854 ms at 702,464 ideal cycles further reveals that Conv1—a
 892 relatively small 7 × 7 convolution with 64 output channels—leaves
 893 significant PE resources idle. For deeper layers with more channels
 894 and smaller spatial dimensions, utilization would increase, making
 895 Timeloop’s per-layer analysis essential for identifying which layers
 896 bottleneck the full-model pipeline. This layer-by-layer decomposi-
 897 tion is a capability unique to analytical accelerator models and
 898 unavailable in GPU-targeting tools like NeuSight.

899 Absolute verification requires RTL simulation or silicon mea-
 900 surement.

901 **7.5 nn-Meter: Complete Failure**

902 nn-Meter claims <1% MAPE—the lowest reported error among all
 903 surveyed tools. After four deployment attempts (>4 hours), we ob-
 904 tained **zero predictions**: pre-trained models serialized with scikit-
 905 learn 0.23.1 (2020) cannot be deserialized with current versions.
 906 Predictors cover Cortex-A76 CPU, Adreno 630/640 GPU, and Myri-
 907 ad VPU, but none are functional. **The tool claiming the best**
 908 **accuracy is the only tool that produces no output**—pickle
 909 serialization without version pinning created an expiration date,
 910 rendering the tool unusable within two years. The failure mode is in-
 911 structive: nn-Meter’s kernel-detection approach segments a model
 912 graph into fusible subgraphs, then predicts each subgraph’s latency
 913 using a pre-trained random forest. The model weights were serial-
 914 ized using Python’s pickle module, which offers no cross-version
 915 compatibility guarantees. When scikit-learn’s internal represen-
 916 tation changed (versions 0.23→1.0+), all four predictors became
 917 unloadable. This failure pattern—functional at publication time
 918 but broken within the maintenance window—is likely widespread
 919 across ML-augmented tools that rely on serialized model weights
 920 without containerized environments. Beyond the serialization is-
 921 sue, nn-Meter’s architecture reveals a deeper problem: the kernel
 922 detection algorithm that segments computation graphs into fusible
 923 graphs.

Table 9: Tool coverage of LLM benchmark suite (28 scenarios).
S=Supported, P=Partial, U=Unsupported. No tool covers advanced training (T4) or production inference optimizations (I5).

Category	#	Neu.	AST.	VID.	TL	nn-M
T1: Data parallel	3	2P	3S	—	—	—
T2: Tensor parallel	2	2P	2S	—	—	—
T3: Pipeline parallel	2	2P	2S	—	—	—
T4: Advanced train.	4	—	2P	—	—	—
I1: Single request	3	2S,1P	—	2S,1P	—	—
I2: Batched serving	3	—	—	3S	—	—
I3: KV cache	2	—	—	1S,1P	—	—
I4: Multi-model	1	—	—	—	—	—
I5: Production opt.	4	—	—	—	—	—
Supported	5	7	6	0	0	0
Partial	3	2	2	0	0	0
Coverage	18%	25%	21%	0%	0%	0%

subgraphs was validated only on CNN architectures (ResNet, MobileNet, EfficientNet). Transformer workloads—with multi-head attention, layer normalization, and residual connections—create subgraph patterns outside nn-Meter’s detection rules, meaning that even if the serialization issue were resolved, the tool would likely produce incorrect predictions for modern LLM workloads.

7.6 Benchmark Suite Coverage

Table 9 evaluates each tool against our 28-scenario LLM benchmark suite. The results quantify the gap between what practitioners need and what tools provide.

Half of LLM workloads have zero tool coverage. Of 28 scenarios, 14 (50%) are not addressable by any evaluated tool. The entirely uncovered scenarios include FP8 mixed-precision training (T4.1), LoRA fine-tuning (T4.2), speculative decoding (I5.1), prefix caching (I5.2), INT4 quantized inference (I5.3), disaggregated serving (I5.4), and multi-model co-location (I4.1). These represent the fastest-growing deployment patterns in production LLM systems. Sequence parallelism (T4.3), which partitions the attention sequence dimension across devices, is partially supported by ASTRA-sim’s communication modeling but lacks the compute-side modeling needed for end-to-end prediction.

Tools cover disjoint slices with minimal overlap. ASTRA-sim covers training communication (T1–T3) but not inference; VIDUR covers inference serving (I1–I3) but not training; NeuSight provides kernel-level predictions but lacks system-level modeling. Only 3 scenarios (I1.1, I1.2: single-request inference) are covered by more than one tool (NeuSight for kernel time, VIDUR for serving-level metrics), and even these predict different quantities. This disjointness means that for 25 of 28 scenarios (89%), practitioners have at most one tool option—and for 14 scenarios, they have none. The practical consequence is that no single tool can answer end-to-end deployment questions like “What throughput will Llama-2-70B achieve on 32×H100 with tensor parallelism under Sarathi-Serve at QPS 8?”—answering this requires combining NeuSight’s kernel predictions with ASTRA-sim’s communication modeling and VIDUR’s

scheduling simulation, a composition that no existing framework supports.

Modern techniques are the largest gap. Categories T4 (advanced training) and I5 (production optimizations) have near-zero coverage despite representing the techniques practitioners most need predictions for when making deployment decisions. MoE expert parallelism (T4.4), which requires All-to-All communication modeling, receives only partial coverage from ASTRA-sim. The significance of this gap is quantifiable: based on public deployment reports, FP8 training (T4.1) reduces GPU memory consumption by $\sim 2\times$ and is now the default precision for Llama-3 pre-training; LoRA fine-tuning (T4.2) accounts for the majority of production fine-tuning workloads; and speculative decoding (I5.1) is deployed in production at multiple LLM serving providers. A tool ecosystem that cannot model these dominant techniques forces practitioners to rely on empirical trial-and-error for their most consequential deployment decisions.

Per-scenario gap analysis. The 14 entirely uncovered scenarios cluster into three groups. *Training-side gaps* (T4.1–T4.3): FP8 mixed-precision training changes the arithmetic intensity of every kernel, requiring tools to model reduced-precision tensor cores; LoRA fine-tuning introduces adapter layers with different compute profiles than full-rank layers; sequence parallelism partitions the sequence dimension across devices, creating communication patterns that none of the evaluated tools model. *Inference-side gaps* (I5.1–I5.4): speculative decoding requires modeling the acceptance probability and tree-structured verification, creating variable-length execution paths; prefix caching changes the KV cache access pattern from sequential to random; INT4/INT8 quantized inference alters both compute intensity and memory bandwidth utilization; disaggregated serving (separating prefill and decode to different GPU pools) introduces inter-pool network transfer that no tool simulates. *Multi-model gaps* (I4.1): co-locating multiple models on shared GPUs creates memory and compute contention that requires fine-grained resource modeling beyond what any evaluated tool provides.

Failure mode taxonomy for uncovered scenarios. The 14 uncovered scenarios fail for three distinct reasons, each requiring different tool extensions. *Missing algorithmic primitives*: speculative decoding (I5.1) and prefix caching (I5.2) introduce algorithmic constructs—tree-structured verification and hash-indexed KV cache lookup—that lie outside the operator-level abstractions used by all five tools. Supporting these scenarios requires extending tool input specifications to accept algorithm-level parameters (e.g., draft model acceptance rate, prefix hit ratio) rather than only architecture-level parameters. *Missing hardware models*: FP8 training (T4.1) and INT4 inference (I5.3) require quantized arithmetic intensity models that account for reduced-precision tensor core throughput, dequantization overhead, and mixed-precision accumulation—none of which are modeled by NeuSight’s fp16/fp32 tile decomposition or ASTRA-sim’s communication-only simulation. *Missing system-level interactions*: disaggregated serving (I5.4) and multi-model co-location (I4.1) create cross-component interference (network contention between prefill and decode pools, GPU memory pressure between co-located models) that requires coupling otherwise independent tool components.

Coverage concentration. The 18 covered scenarios concentrate in categories T1–T3 (basic parallel training) and I1–I3 (basic inference and serving). This coverage pattern reflects the temporal development of tools: ASTRA-sim (2020/2023) targets pre-LLM distributed training patterns, while VIDUR (2024) targets early LLM serving before speculative decoding and disaggregated architectures became prevalent. The field’s tool development lags deployment practice by 1–2 years. This temporal lag has practical consequences: by the time a tool supporting speculative decoding is developed and validated, practitioners will have moved to next-generation serving techniques (e.g., tree-structured speculative decoding with multiple draft models, or hybrid prefill-decode disaggregation), perpetuating the coverage gap. Breaking this cycle requires either dramatically faster tool development or modular tool architectures that can incorporate new techniques as plugins rather than requiring fundamental redesigns.

Aggregate coverage by tool. Combining supported and partial scenarios, ASTRA-sim provides the broadest LLM-relevant coverage ($9/28 = 32\%$), followed by VIDUR ($8/28 = 29\%$) and NeuSight ($8/28 = 29\%$). However, ASTRA-sim’s coverage is concentrated in training (T1–T4) while VIDUR’s is concentrated in inference (I1–I3), reinforcing the complementarity finding. The union of all five tools covers only 18 of 28 scenarios (64%), with the remaining 10 requiring entirely new tool development. Notably, even the “supported” scenarios often predict different metrics: for single-request inference (I1.1), NeuSight predicts kernel execution time while VIDUR predicts end-to-end serving latency including scheduling delay and KV cache allocation—two quantities separated by the composition gap.

Coverage quality varies within “supported” scenarios. Even among the 18 covered scenarios, support quality is uneven. For T1.1 (data-parallel GPT-2 on $8 \times A100$), NeuSight provides only per-GPU kernel time (partial) while ASTRA-sim provides full communication modeling (supported)—but neither tool produces the end-to-end iteration time that practitioners optimize. For I2.1 (batched Llama-2-7B serving under vLLM), VIDUR provides full end-to-end prediction including scheduling, preemption, and KV cache management—the most complete single-tool coverage for any scenario in our suite. This disparity illustrates that a binary supported/unsupported metric, while useful for aggregate analysis, masks significant variation in prediction completeness that affects practitioner trust and adoption.

7.7 Cross-Cutting Findings

Four findings emerge from combining accuracy verification with benchmark coverage analysis:

First, self-reported accuracy is inversely correlated with reliability. By claimed accuracy: nn-Meter (<1%) > NeuSight (2.3%) > VIDUR (<5%) > Timeloop (5–10%) > ASTRA-sim (5–15%). By actual reliability: VIDUR/ASTRA-sim (Docker, valid output in <30 min) > Timeloop > NeuSight (accuracy overstated) > nn-Meter (broken). The tools claiming the lowest error are the least reliable.

Second, the five tools are complementary, not competing. No two tools meaningfully overlap: NeuSight predicts GPU kernels; ASTRA-sim simulates communication; VIDUR models LLM serving;

Timeloop explores accelerator design; nn-Meter targets edge. The field needs a unified pipeline combining tool strengths (Section 8).

Third, the composition gap dominates end-to-end error. NeuSight’s kernel-level 5–9% MAPE grows to 10–28% at model level. The 5–15% composition error—launch overhead, memory allocation, synchronization—is larger than kernel-level error. Improving kernel predictors has diminishing returns until composition is solved (Figure 4).

Fourth, 50% of modern LLM workloads lack any modeling tool. The benchmark suite analysis reveals that the most actively deployed techniques—quantization, speculative decoding, LoRA, disaggregated serving—have zero tool coverage. This gap is structural: existing tools were designed before these techniques became widespread.

Fifth, deployment robustness varies inversely with model complexity. Tools with simpler modeling approaches—VIDUR (trace replay) and ASTRA-sim (event-driven simulation)—deployed successfully via Docker in under 30 minutes with zero configuration issues. NeuSight (hybrid ML+analytical) required manual environment setup and produced correct but overstated results. nn-Meter (pure ML-augmented) failed entirely. Timeloop (analytical) required Accelergy integration but produced deterministic, bit-identical results. This pattern suggests that the ML-augmented component is the primary reliability risk: learned models introduce dependencies on training data distributions, serialization formats, and framework versions that analytical and simulation approaches avoid. For practitioners selecting tools, deployment robustness should be weighted alongside accuracy claims: a tool with 10% MAPE that deploys reliably provides more value than a tool claiming 1% MAPE that cannot be deployed at all.

Sixth, inference and training accuracy diverge systematically. Across NeuSight’s 146 configurations, inference accuracy (mean MAPE: 5.87–27.10% depending on device) is consistently better than training accuracy for NVIDIA GPUs (V100: 5.87% inf vs. 8.91% train; A100-80G: 8.63% inf vs. 7.59% train is the only exception). For AMD GPUs, the gap is larger: MI100 shows 10.80% inference vs. 15.62% training; MI210 shows 8.40% vs. 15.73%. Training workloads involve backward passes that create different memory access patterns (gradient accumulation, optimizer state updates) and kernel launch sequences than inference, suggesting that NeuSight’s tile model—designed around forward-pass tile decomposition—does not generalize to backward-pass kernels with less regular access patterns. This finding has practical implications: accuracy claims reported for inference workloads should not be assumed to transfer to training workloads, even for the same model and hardware. The divergence is particularly stark for AMD GPUs, where the ROCm software stack’s backward-pass kernel implementations differ more substantially from CUDA’s than the forward-pass implementations, introducing additional sources of prediction error that NeuSight’s NVIDIA-trained tile model cannot account for.

Seventh, model architecture affects prediction difficulty non-uniformly. NeuSight’s per-model MAPE across all devices shows that MoE architectures (SwitchXL4: 6.33–17.65% APE range across configurations) exhibit higher variance than dense models (OPT-13B: 0.38–10.53%; GPT-3-2.7B: 0.43–7.73%). The higher variance for MoE arises because expert routing creates workload-dependent computation patterns that a static tile decomposition

Table 10: Deployment experience for each evaluated tool.
Time excludes download. Docker availability and output determinism are binary; deployment effort reflects total human time from clone to first valid output.

Tool	Docker	Time	Determ.	Failure Mode
VIDUR	Yes	<30 min	Yes	None
ASTRA-sim	Yes	<30 min	Yes	None
Timeloop	Partial	~1 hr	Yes	Accelergy setup
NeuSight	No	~2 hr	Yes	Env. config
nn-Meter	No	4+ hr	N/A	Serialization

cannot fully capture. This observation extends to future tools: MoE, sparse attention, and dynamic architectures will likely require workload-aware prediction mechanisms rather than architecture-only models.

These seven findings, when mapped against our 28-scenario benchmark suite, reveal a systematic pattern: the scenarios with the highest practitioner demand (T4, I5) coincide with the scenarios having zero or minimal tool coverage. Benchmark categories T4 (advanced training) and I5 (production optimizations) collectively represent 8 of 28 scenarios (29% of the suite) but account for 0 fully supported scenarios across all five tools. Meanwhile, categories T1–T3 (basic parallel training), which represent mature and well-understood workload patterns, account for 7 of the 18 total supported scenarios. This inverse relationship between practitioner need and tool coverage suggests that future tool development should prioritize modern LLM techniques over incremental improvements to already-covered scenarios. Concretely, a tool achieving even 20% MAPE on speculative decoding (I5.1) or disaggregated serving (I5.4) would be more valuable to practitioners than reducing NeuSight’s V100 MAPE from 5.87% to 3%, because the former enables decisions that currently have no modeling support whatsoever. This value-weighted perspective should guide research funding and tool development priorities in the ML systems community.

7.8 Deployment Experience and Reproducibility

Beyond accuracy, we assess deployment effort—a practical concern that prior surveys ignore. Table 10 summarizes our experience deploying each tool from scratch.

Docker availability is the strongest predictor of deployment success. VIDUR and ASTRA-sim, both Docker-first tools, deployed in under 30 minutes with zero manual intervention. Timeloop required partial manual setup for its Accelergy energy estimation plugin but produced results within one hour. NeuSight required manual Python environment configuration and model weight downloads but eventually succeeded. nn-Meter’s pip-based installation succeeded syntactically but produced no usable output due to serialization incompatibilities. This represents the worst deployment outcome: silent success at install time masking complete failure at inference time, with no diagnostic error message until the user attempts to load a predictor—a failure pattern that undermines trust in the broader ML-augmented tool ecosystem.

Determinism varies by methodology. All evaluated tools except nn-Meter (which produced no output) generated bit-identical

results across three independent runs on the same platform. This determinism is notable for NeuSight, whose hybrid ML+analytical approach could in principle exhibit stochastic behavior; the determinism arises because NeuSight uses fixed pre-trained weights and analytical tile decomposition with no stochastic inference-time components. Deterministic outputs simplify regression testing and enable exact reproducibility—properties that should be standard but are not guaranteed by ML-augmented tools that use stochastic inference (e.g., dropout at test time, Monte Carlo sampling for uncertainty quantification).

7.9 Threats to Validity

External validity. Our venue-focused search may under-represent industry tools. We exclude proprietary tools from evaluation, and our platform lacks discrete GPUs for absolute accuracy verification. The benchmark suite’s 28 scenarios, while representative, cannot cover every production deployment pattern; emerging workloads (e.g., retrieval-augmented generation, multi-modal models) are not yet included.

Internal validity. Our evaluation covers 5 of 22 tools. Findings rest on single tool instances per methodology type—e.g., nn-Meter may be unrepresentative due to deployment failure. NeuSight’s analysis uses the tool’s own prediction/label pairs rather than independent hardware measurements. The per-device sample sizes vary (3–18 configurations), limiting statistical power for devices with few data points (e.g., P4 with only 3 configurations, A100-SXM with 3 configurations). We mitigate this by reporting both mean and worst-case APE. Our benchmark suite covers 28 scenarios, but the distribution is not uniform: training scenarios (11) outnumber inference scenarios (13), with MoE and multi-model scenarios (T4.4, I4.1) represented by only one scenario each. A more balanced suite might weight scenarios by practitioner frequency of use, but such weighting data is not publicly available. Despite these limitations, our suite provides the first standardized coverage metric for ML performance tools, enabling future evaluations to quantitatively compare tool ecosystems.

Construct validity. Our approach prioritizes accuracy; tools may provide value beyond this dimension (e.g., Timeloop’s energy breakdown for design insight, ASTRA-sim’s what-if analysis for topology exploration). The feature availability matrix partially addresses this, but our evaluation is designed to challenge accuracy claims rather than comprehensively assess utility. Additionally, our coverage criterion (supported/partial/unsupported) does not capture the quality of partial support—ASTRA-sim’s partial coverage of MoE training (T4.4), for example, provides All-to-All communication modeling but misses expert load balancing effects. A finer-grained coverage metric—e.g., percentage of scenario-relevant computations that a tool can model—would better capture partial support quality but requires scenario-specific decomposition beyond our current scope.

Temporal validity. Our evaluation reflects tool state as of January 2026. Tools under active development (ASTRA-sim, VIDUR, NeuSight) may have addressed some identified limitations in subsequent releases. However, our core findings about structural coverage gaps and accuracy overstatement reflect fundamental design

1277 choices rather than fixable bugs, and are likely to persist across versions.
 1278 We encourage future evaluations to adopt our independent verification methodology and benchmark suite to enable longitudinal tracking of tool accuracy. The benchmark suite itself should
 1280 evolve as new LLM techniques emerge; we provide it as a living document in the supplementary material.

1281 **Benchmark suite validity.** Our 28-scenario benchmark suite
 1282 was designed around the LLM workload landscape as of early 2026.
 1283 Emerging techniques not represented include retrieval-augmented
 1284 generation (RAG), which introduces variable-length retrieval latency into the inference pipeline; multi-modal models combining
 1285 vision encoders with language models, which create heterogeneous
 1286 compute patterns; and reinforcement learning from human feedback
 1287 (RLHF), which requires modeling reward model inference
 1288 interleaved with policy updates. We designed the suite to be extensible:
 1289 each scenario is specified by a tuple of (model architecture,
 1290 hardware configuration, parallelism strategy, target metric),
 1291 allowing new scenarios to be added as techniques mature without
 1292 restructuring the evaluation framework. Future versions should
 1293 expand to at least 40 scenarios to maintain coverage as the LLM
 1294 deployment landscape diversifies.

1295 8 Toward a Unified Simulation Pipeline

1300 The feature matrix (Table 5) reveals disjoint coverage: no single
 1301 tool spans kernel execution through distributed training to serving
 1302 SLAs. We propose a five-layer pipeline composing predictions
 1303 hierarchically:

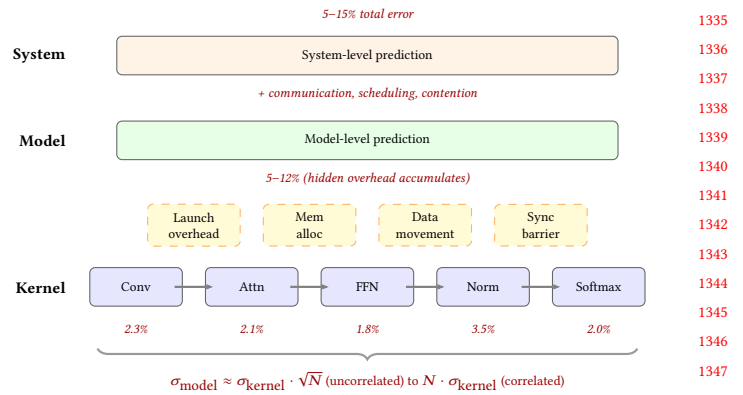
- 1306 (1) **Hardware design** (Timeloop): Explore dataflow/mapping
 1307 design space for per-layer energy and latency on custom
 1308 accelerators.
- 1309 (2) **Kernel prediction** (NeuSight / Timeloop): Predict per-
 1310 kernel execution time on GPUs (12 types) or custom archi-
 1311 tectures.
- 1312 (3) **Model composition (CRITICAL GAP)**: Compose kernel
 1313 predictions into full iteration time, accounting for launch
 1314 overhead, memory allocation, and data movement. *No ex-*
1315 isting tool validates this layer.
- 1316 (4) **Distributed training** (ASTRA-sim): Simulate multi-GPU
 1317 communication, collectives, and topology effects for train-
 1318 ing throughput.
- 1319 (5) **Serving system** (VIDUR): Model request scheduling, batch-
 1320 ing, KV cache, and queuing for TTFT/TPOT prediction.

1322 **The critical gap: kernel-to-model composition.** NeuSight's
 1323 5–9% kernel MAPE grows to 10–28% at model level via launch over-
 1324 head ($\sim 5\text{--}10 \mu\text{s/kernel}$), inter-kernel data movement, and synchronization—
 1325 a gap *larger than kernel-level error*.

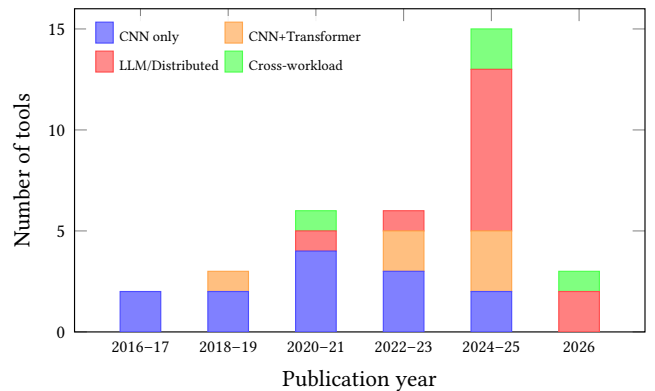
1326 **Integration requirements.** Realizing this pipeline requires:
 1327 (a) a common workload format; (b) validated composition models
 1328 with formal error bounds; and (c) cross-hardware transfer methods
 1329 (accuracy degrades 3–4× outside training distributions).

1331 9 Open Challenges and Future Directions

1332 Our evaluation exposes six research directions.



1333 **Figure 4: Error composition: kernel predictions (2–3%) accu-
 1334 mulate to 5–12% model-level and 5–15% system-level error.**



1335 **Figure 5: Workload coverage by publication period. MoE and
 1336 diffusion models remain uncharacterized.**

1337 **1. Bridging the composition gap.** Kernel errors of 2–3% yield
 1338 5–12% model-level error (Figure 4; $\sigma_{\text{model}} \approx \sigma_{\text{kernel}} \cdot \sqrt{N}$ uncorre-
 1339 lated, linear when correlated), yet no validated composition pipeline
 1340 exists.

1341 **2. Frontier workload coverage.** MoE, diffusion [37], and dy-
 1342 namic inference lack validated tools; scaling laws [12, 20, 25, 34]
 1343 predict loss but not latency (Figure 5).

1344 **3. Hardware transfer.** Cross-family transfer (GPU→TPU→PIM)
 1345 remains unsolved; PIM [24, 29, 42, 54], chiplets, and disaggregated
 1346 designs blur memory hierarchy assumptions.

1347 **4. Network simulation fidelity.** Current tools [45, 79] use ana-
 1348 lytical network abstractions, omitting packet-level congestion and
 1349 tail-latency effects captured by NS-3 [65] at orders-of-magnitude
 1350 slowdown. Quantifying when packet-level fidelity matters for ML
 1351 collectives remains unexplored.

1352 **5. Standardized evaluation infrastructure.** No MLPerf [49,
 1353 64] equivalent exists for prediction; the community needs common
 1354 benchmarks, portable formats (ONNX, Chakra [70]), and Docker-
 1355 first deployment.

1393 **6. Temporal stability.** Software evolution (FlashAttention [14],
 1394 CUDA updates) silently invalidates models; nn-Meter’s failure within
 1395 two years underscores the need for continuous validation [63].

1396 10 Conclusion

1398 We survey 22 ML performance modeling tools and independently
 1399 evaluate five against a 28-scenario LLM benchmark suite. Self-
 1400 reported accuracy is unreliable (NeuSight: 2.3% claimed vs. 5.87–
 1401 27.10% measured; nn-Meter: no output). The five tools are com-
 1402 plementary but disjoint, motivating a unified pipeline—yet the
 1403 5–15% kernel-to-model composition gap exceeds kernel-level error,
 1404 and 50% of modern LLM techniques lack any tool support. The
 1405 most pressing needs are validated composition models, benchmark-
 1406 driven development for uncovered scenarios, and continuous vali-
 1407 dation.

1409 References

- [1] Martín Abadi, Paul Barham, Jianmin Chen, Zhifeng Chen, Andy Davis, Jeffrey Dean, Matthieu Devin, Sanjay Ghemawat, Geoffrey Irving, Michael Isard, et al. 2016. TensorFlow: A System for Large-Scale Machine Learning. In *Proceedings of the 12th USENIX Symposium on Operating Systems Design and Implementation (OSDI)*. 265–283.
- [2] Amey Agrawal, Nitin Kedia, Ashish Panwar, Jayashree Mohan, Nipun Kwatra, Bhargav S. Gulavani, Alexey Tumanov, and Ramachandran Ramachandran. 2024. Taming Throughput-Latency Tradeoff in LLM Inference with Sarathi-Serve. In *Proceedings of the 18th USENIX Symposium on Operating Systems Design and Implementation (OSDI)*. 117–134.
- [3] Amey Agrawal, Ashish Panwar, Jayashree Mohan, Nipun Kwatra, Bhargav S. Gulavani, and Ramachandran Ramachandran. 2024. VIDUR: A Large-Scale Simulation Framework for LLM Inference. In *Proceedings of Machine Learning and Systems (MLSys)*. 1–15.
- [4] Ali Bakhoda, George L. Yuan, Wilson W. L. Fung, Henry Wong, and Tor M. Aamodt. 2009. Analyzing CUDA Workloads Using a Detailed GPU Simulator. In *Proceedings of the IEEE International Symposium on Performance Analysis of Systems and Software (ISPASS)*. 163–174. <https://doi.org/10.1109/ISPASS.2009.4919648>
- [5] Abhimanyu Rajeshkumar Bambhaniya et al. 2025. HERMES: Understanding and Optimizing Multi-Stage AI Inference Pipelines. *arXiv preprint arXiv:2504.09775* (2025). Heterogeneous multi-stage LLM inference simulator with analytical modeling.
- [6] Nathan Binkert, Bradford Beckmann, Gabriel Black, Steven K. Reinhardt, Ali Saidi, Arkaprava Basu, Joel Hestness, Derek R. Hower, Tushar Krishna, Somayeh Sardashti, Rathijit Sen, Korey Sewell, Muhammad Shoaib, Nilay Vaish, Mark D. Hill, and David A. Wood. 2011. The gem5 Simulator. *ACM SIGARCH Computer Architecture News* 39, 2 (2011), 1–7. <https://doi.org/10.1145/2024716.2024718>
- [7] Kai Cai, Wei Miao, Junyu Zhu, Jiaxu Chen, Hao Shan, Huanyu Li, and Chi Zhang. 2024. Echo: Simulating Distributed Training At Scale. *arXiv preprint arXiv:2412.12487* (2024).
- [8] Zheng Cao et al. 2025. AMALI: An Analytical Model for Accurately Modeling LLM Inference on Modern GPUs. In *Proceedings of the 52nd Annual International Symposium on Computer Architecture (ISCA)*. 1–14. <https://doi.org/10.1145/3695053.3731064> Reduces GPU LLM inference MAPE from 127.56% to 23.59% vs GCoM baseline.
- [9] Tianshi Chen, Zidong Du, Ninghui Sun, Jia Wang, Chengyong Wu, Yunji Chen, and Olivier Temam. 2014. DianNao: A Small-Footprint High-Throughput Accelerator for Ubiquitous Machine-Learning. In *Proceedings of the 19th International Conference on Architectural Support for Programming Languages and Operating Systems (ASPLOS)*. 269–284. <https://doi.org/10.1145/2541940.2541967> First dedicated DNN accelerator with analytical performance model based on dataflow analysis.
- [10] Tianqi Chen, Thierry Moreau, Ziheng Jiang, Lianmin Zheng, Eddie Yan, Meghan Cowan, Haichen Shen, Leyuan Wang, Yuwei Hu, Luis Ceze, Carlos Guestrin, and Arvind Krishnamurthy. 2018. TVM: An Automated End-to-End Optimizing Compiler for Deep Learning. In *Proceedings of the 13th USENIX Symposium on Operating Systems Design and Implementation (OSDI)*. 578–594.
- [11] Yu-Hsin Chen, Joel Emer, and Vivienne Sze. 2016. Eyeriss: A Spatial Architecture for Energy-Efficient Dataflow for Convolutional Neural Networks. In *Proceedings of the 43rd International Symposium on Computer Architecture (ISCA)*. 367–379. <https://doi.org/10.1109/ISCA.2016.40>
- [12] Leshem Choshen, Yang Zhang, and Jacob Andreas. 2025. A Hitchhiker’s Guide to Scaling Law Estimation. In *Proceedings of the 42nd International Conference on Machine Learning (ICML)*. 1–25. Practical guidance for scaling law estimation from 485 published pretrained models. IBM/MIT.
- [13] Weiwei Chu, Xinfeng Xie, Jiecao Yu, Jie Wang, Pavan Balaji, Ching-Hsiang Chu, Jongsoo Park, et al. 2025. Scaling Llama 3 Training with Efficient Parallelism Strategies. In *Proceedings of the 52nd Annual International Symposium on Computer Architecture (ISCA)*. 1–15. 4D parallelism for Llama 3 405B on 16K H100 GPUs. Achieves 400 TFLOPS/GPU. Meta.
- [14] Tri Dao, Dan Fu, Stefano Ermon, Atri Rudra, and Christopher Ré. 2022. FlashAttention: Fast and Memory-Efficient Exact Attention with IO-Awareness. In *Advances in Neural Information Processing Systems (NeurIPS)*, Vol. 35. 16344–16359.
- [15] Lukasz Dudziak, Thomas Chau, Mohamed S. Abdelfattah, Royson Lee, Hyeji Kim, and Nicholas D. Lane. 2024. Latency Predictors for Neural Architecture Search. In *Proceedings of Machine Learning and Systems (MLSys)*. 1–14.
- [16] Yang Feng, Zhehao Li, Jiacheng Yang, and Yunxin Liu. 2024. LitePred: Transferable and Scalable Latency Prediction for Hardware-Aware Neural Architecture Search. In *Proceedings of the 21st USENIX Symposium on Networked Systems Design and Implementation (NSDI)*. 1–18.
- [17] Paraskevas Gavrilidis et al. 2025. LIFE: Forecasting LLM Inference Performance via Hardware-Agnostic Analytical Modeling. *arXiv preprint arXiv:2508.00904* (2025). Hardware-agnostic analytical model for LLM inference performance forecasting.
- [18] Siddharth Ghosh et al. 2025. Frontier: Simulating the Next Generation of LLM Inference Systems. *arXiv preprint arXiv:2508.03148* (2025). Stage-centric simulator for MoE and disaggregated LLM inference, models expert parallelism and cross-cluster routing.
- [19] Alicia Golden et al. 2025. PRISM: Probabilistic Runtime Insights and Scalable Performance Modeling for Large-Scale Distributed Training. *arXiv preprint arXiv:2510.15596* (2025). Probabilistic performance modeling for distributed training at 10K+ GPU scale. Meta.
- [20] Alexander Hagele, Elie Bakouch, Atli Kosson, Loubna Ben Allal, Leandro Von Werra, and Martin Jaggi. 2024. Scaling Laws and Compute-Optimal Training Beyond Fixed Training Durations. In *Advances in Neural Information Processing Systems (NeurIPS)*, Vol. 37. Spotlight. Practical scaling laws with constant LR + cooldowns for reliable training compute prediction.
- [21] Ameer Haj-Ali et al. 2025. Omnipwise: Predicting GPU Kernels Performance with LLMs. *arXiv preprint arXiv:2506.20886* (2025). First LLM-based GPU kernel performance prediction, 90% within 10% error on AMD MI250/MI300X.
- [22] Yanbin Hao et al. 2025. POD-Attention: Unlocking Full Prefill-Decode Overlap for Faster LLM Inference. In *Proceedings of the 30th ACM International Conference on Architectural Support for Programming Languages and Operating Systems (ASPLOS)*. 1–15. Full overlap between prefill and decode phases for LLM inference.
- [23] John L. Hennessy and David A. Patterson. 2019. A New Golden Age for Computer Architecture. *Commun. ACM* 62, 2 (2019), 48–60. <https://doi.org/10.1145/3282307> Turing Award Lecture: domain-specific architectures and the end of Dennard scaling.
- [24] Guseul Heo, Sangyeop Lee, Jaehong Cho, Hyunmin Choi, Sanghyeon Lee, Hyungkyu Ham, Gwangsun Kim, Divya Mahajan, and Jongse Park. 2024. NeupIMs: NPU-PIM Heterogeneous Acceleration for Batched LLM Inferencing. In *Proceedings of the 29th ACM International Conference on Architectural Support for Programming Languages and Operating Systems (ASPLOS)*. 1–17. NPU-PIM heterogeneous architecture for LLM inference with performance modeling. KAIST/Georgia Tech..
- [25] Jordan Hoffmann, Sebastian Borgeaud, Arthur Mensch, Elena Buchatskaya, Trevor Cai, Eliza Rutherford, Diego de Las Casas, Lisa Anne Hendricks, Johannes Welbl, Aidan Clark, et al. 2022. Training Compute-Optimal Large Language Models. *arXiv preprint arXiv:2203.15556* (2022). Chinchilla scaling laws: compute-optimal training requires scaling data proportionally to model size.
- [26] Samuel Hsia, Kartik Chandra, and Kunlu Olukotun. 2024. MAD Max Beyond Single-Node: Enabling Large Machine Learning Model Acceleration on Distributed Systems. In *Proceedings of the 51st Annual International Symposium on Computer Architecture (ISCA)*. 753–766. <https://doi.org/10.1109/ISCA59077.2024.00064>
- [27] Yanping Huang, Youlong Cheng, Ankur Bapna, Orhan Firat, Dehao Chen, Mia Xu Chen, Hyoukjoong Lee, Jiquan Ngiam, Quoc V. Le, Yonghui Wu, and Zhifeng Chen. 2019. GPipe: Efficient Training of Giant Neural Networks using Pipeline Parallelism. In *Advances in Neural Information Processing Systems (NeurIPS)*, Vol. 32. 103–112.
- [28] Rodrigo Huerta, Mojtaba Abaie Shoushtary, Jose-Lorenzo Cruz, and Antonio Gonzalez. 2025. Dissecting and Modeling the Architecture of Modern GPU Cores. In *Proceedings of the 58th IEEE/ACM International Symposium on Microarchitecture (MICRO)*. 369–384. Reverse-engineers modern NVIDIA GPU cores, improves Accel-Sim to 13.98% MAPE. UPC Barcelona..
- [29] Bongjoon Hyun, Taehun Kim, Dongjae Lee, and Minsoo Rhu. 2024. Pathfinding Future PIM Architectures by Demystifying a Commercial PIM Technology. In *Proceedings of the IEEE International Symposium on High Performance Computer Architecture (HPCA)*. 1–15. uPIMulator: cycle-accurate PIM simulation framework for UPMEM. KAIST..

- [1509] [30] Anand Jayarajan, Wei-Lin Hu, Gauri Zhao, and Gennady Pekhimenko. 2023. Sia: Heterogeneity-aware, Goodput-optimized ML-Cluster Scheduling. In *Proceedings of the 29th Symposium on Operating Systems Principles (SOSP)*. 642–657. <https://doi.org/10.1145/3600006.3613175> Extends goodput optimization to heterogeneous GPU clusters for training workloads.
- [1510] [31] Norman P. Jouppi, Doe Hyun Yoon, George Kurian, Sheng Li, Nishant Patil, James Laudon, Cliff Young, and David Patterson. 2023. TPU v4: An Optically Reconfigurable Supercomputer for Machine Learning with Hardware Support for Embeddings. *Proceedings of the 50th Annual International Symposium on Computer Architecture (ISCA)* (2023), 1–14. <https://doi.org/10.1145/3579371.3589350> 4096-chip pods with 3D optical interconnect; up to 1.7x/2.1x faster than TPU v3.
- [1511] [32] Norman P. Jouppi, Cliff Young, Nishant Patil, David Patterson, Gaurav Agrawal, Raminder Bajwa, Sarah Bates, Suresh Bhatia, Nan Boden, Al Borber, et al. 2017. In-Datacenter Performance Analysis of a Tensor Processing Unit. In *Proceedings of the 44th Annual International Symposium on Computer Architecture (ISCA)*. 1–12. <https://doi.org/10.1145/3079856.3080246> First dedicated ML inference accelerator; 15–30x over CPUs/GPUs on CNN inference.
- [1512] [33] Andreas Kosmas Kakolyris, Dimosthenis Masouros, Petros Vavaroutsos, Sotirios Xydis, and Dimitrios Soudris. 2025. throtLL'eM: Predictive GPU Throttling for Energy Efficient LLM Inference Serving. In *Proceedings of the IEEE International Symposium on High Performance Computer Architecture (HPCA)*. 1–14. Achieves up to 43.8% lower energy consumption for LLM inference.
- [1513] [34] Jared Kaplan, Sam McCandlish, Tom Henighan, Tom B. Brown, Benjamin Chess, Rewon Child, Scott Gray, Alec Radford, Jeffrey Wu, and Dario Amodei. 2020. Scaling Laws for Neural Language Models. *arXiv preprint arXiv:2001.08361* (2020). Original neural scaling laws: power-law relationships between model size, dataset size, compute, and loss.
- [1514] [35] Mahmoud Khairy, Zhesheng Shen, Tor M. Aamodt, and Timothy G. Rogers. 2020. Accel-Sim: An Extensible Simulation Framework for Validated GPU Modeling. In *Proceedings of the 47th International Symposium on Computer Architecture (ISCA)*. 473–486. <https://doi.org/10.1109/ISCA45697.2020.00047>
- [1515] [36] JungHo Kim et al. 2025. PyTorchSim: A Comprehensive, Fast, and Accurate NPU Simulation Framework. In *Proceedings of the 58th IEEE/ACM International Symposium on Microarchitecture (MICRO)*. 1–14. <https://doi.org/10.1145/3725843.3756045> PyTorch 2-integrated NPU simulator with custom RISC-V ISA and Tile-Level Simulation.
- [1516] [37] Jin Kim, Byeongjun Shin, Jinha Chung, and Minsoo Rhu. 2026. The Cost of Dynamic Reasoning: Demystifying AI Agents and Test-Time Scaling from an AI Infrastructure Perspective. In *Proceedings of the IEEE International Symposium on High Performance Computer Architecture (HPCA)*. 1–14. HPCA 2026 (Jan 31–Feb 4, 2026, Las Vegas). First comprehensive system-level analysis of AI agents; quantifies resource usage, latency, and datacenter power consumption.
- [1517] [38] Srivatsan Krishnan, Amir Yazdanbakhsh, Shvetank Prakash, Norman P. Jouppi, Jignesh Parmar, Hyoukjun Kim, James Laudon, and Chandrakan Narayanaswami. 2023. ArchGym: An Open-Source Gymnasium for Machine Learning Assisted Architecture Design. In *Proceedings of the 50th International Symposium on Computer Architecture (ISCA)*. 1–16. <https://doi.org/10.1145/3579371.3589049>
- [1518] [39] Hyoukjun Kwon, Prasanth Chatarasi, Michael Barber, Michael Pellauer, Angshuman Parashar, and Tushar Krishna. 2019. MAESTRO: A Data-Centric Approach to Understand Reuse, Performance, and Hardware Cost of DNN Mappings. In *Proceedings of the 52nd IEEE/ACM International Symposium on Microarchitecture (MICRO)*. 1–14. <https://doi.org/10.1145/3352460.3358292>
- [1519] [40] Woosuk Kwon, Zhuohan Li, Siyuuan Zhuang, Ying Sheng, Lianmin Zheng, Cody Hao Yu, Joseph E. Gonzalez, Hao Zhang, and Ion Stoica. 2023. Efficient Memory Management for Large Language Model Serving with PagedAttention. In *Proceedings of the 29th Symposium on Operating Systems Principles (SOSP)*. 611–626. <https://doi.org/10.1145/3600006.3613165>
- [1520] [41] Chris Lattner, Mehdi Amini, Uday Bondhugula, Albert Cohen, Andy Davis, Jacques Pienaar, River Riddle, Tatiana Shpeisman, Nicolas Vasilache, and Oleksandr Zinenko. 2021. MLIR: Scaling Compiler Infrastructure for Domain Specific Computation. In *Proceedings of the IEEE/ACM International Symposium on Code Generation and Optimization (CGO)*. 2–14. <https://doi.org/10.1109/CGO51591.2021.9370308> Multi-level IR infrastructure enabling cost model composition across abstraction levels.
- [1521] [42] Hyojung Lee, Daehyeon Baek, Jimyoung Son, Jieun Choi, Kihyo Moon, and Minsung Jang. 2025. PAISE: PIM-Accelerated Inference Scheduling Engine for Transformer-based LLM. In *Proceedings of the IEEE International Symposium on High Performance Computer Architecture (HPCA)*. 1–14. PIM-based LLM inference scheduling, 48.3% speedup, 11.5% power reduction. Samsung..
- [1522] [43] Hayeon Lee, Sewooong Lee, Song Chong, and Sung Ju Hwang. 2021. HELP: Hardware-Adaptive Efficient Latency Prediction for NAS via Meta-Learning. In *Advances in Neural Information Processing Systems (NeurIPS)*, Vol. 34. 27016–27028.
- [1523] [44] Seunghyun Lee, Amar Phanishayee, and Divya Mahajan. 2025. NeuSight: GPU Performance Forecasting via Tile-Based Execution Analysis. In *Proceedings of the 30th ACM International Conference on Architectural Support for Programming Languages and Operating Systems (ASPLOS)*. 1–15.
- [1524] [45] Jianbo Li et al. 2025. TrioSim: A Lightweight Simulator for Large-Scale DNN Workloads on Multi-GPU Systems. In *Proceedings of the 52nd Annual International Symposium on Computer Architecture (ISCA)*. 1–13. Multi-GPU DNN simulation with lightweight approach for distributed training analysis.
- [1525] [46] Shang Li, Zhiyuan Yang, Dhiraj Reddy, Ankur Srivastava, and Bruce Jacob. 2020. DRAMsim3: A Cycle-Accurate, Thermal-Capable DRAM Simulator. *IEEE Computer Architecture Letters* 19, 2 (2020), 106–109. <https://doi.org/10.1109/LCA.2020.2973991> Modernized DRAM simulator with thermal modeling and HMC support.
- [1526] [47] Wenxuan Liang et al. 2025. Lumos: Efficient Performance Modeling and Estimation for Large-scale LLM Training. In *Proceedings of Machine Learning and Systems (MLSys)*. 1–16. Trace-driven performance modeling achieving 3.3% error on H100 GPUs for LLM training.
- [1527] [48] Haocong Luo, Yahya Can Tugrul, F. Nisa Bostancı, Ataberk Olgun, A. Giray Yaglikeci, and Onur Mutlu. 2023. Ramulator 2.0: A Modern, Modular, and Extensible DRAM Simulator. *IEEE Computer Architecture Letters* 22, 2 (2023), 129–132. <https://doi.org/10.1109/LCA.2023.3333759> Modular DRAM simulator with DDR5, LPDDR5, HBM3, GDDR6 support and RowHammer mitigation modeling.
- [1528] [49] Peter Mattson, Christine Cheng, Cody Coleman, Greg Diamos, Paulius Micikevicius, David Patterson, Hanlin Tang, Gu-Yeon Wei, Peter Bailis, Victor Bittorf, et al. 2020. MLPerf Training Benchmark. In *Proceedings of Machine Learning and Systems (MLSys)*. 336–349. Standard ML training benchmark suite covering image classification, object detection, NLP, recommendation, reinforcement learning.
- [1529] [50] Azaz-Ur-Rehman Nasir, Samroz Ahmad Shoib, Muhammad Abdullah Hanif, and Muhammad Shafique. 2025. ESM: A Framework for Building Effective Surrogate Models for Hardware-Aware Neural Architecture Search. In *Proceedings of the 62nd ACM/IEEE Design Automation Conference (DAC)*. 1–6. 97.6% accuracy surrogate model framework for HW-aware NAS.
- [1530] [51] Amir Nasr-Esfahany et al. 2025. Concorde: Fast and Accurate CPU Performance Modeling with Compositional Analytical-ML Fusion. In *Proceedings of the 52nd Annual International Symposium on Computer Architecture (ISCA)*. 1–15. Hybrid analytical-ML approach achieving 2% CPI error at 5 orders of magnitude faster than gem5.
- [1531] [52] NVIDIA Corporation. 2019. Nsight Compute: Interactive Kernel Profiler. <https://developer.nvidia.com/nsight-compute>. Industry-standard GPU kernel profiling tool with roofline analysis.
- [1532] [53] Angshuman Parashar, Priyanka Raina, Yukun Sophia Shao, Yu-Hsin Chen, Victor A. Ying, Anurag Muber, Rangharajan Venkatesan, Brueck Khailany, Stephen W. Keckler, and Joel Emer. 2019. Timeloop: A Systematic Approach to DNN Accelerator Evaluation. In *Proceedings of the IEEE International Symposium on Performance Analysis of Systems and Software (ISPASS)*. 304–315. <https://doi.org/10.1109/ISPASS.2019.00042>
- [1533] [54] Jaehyun Park, Jaewan Choi, Kwanhee Kyung, Michael Jaemin Kim, Yongsuk Kwon, Nam Sung Kim, and Jung Ho Ahn. 2024. AttAcc! Unleashing the Power of PIM for Batched Transformer-based Generative Model Inference. In *Proceedings of the 29th ACM International Conference on Architectural Support for Programming Languages and Operating Systems (ASPLOS)*. 1–16. PIM-based accelerator for batched transformer attention. Seoul National University/UIUC..
- [1534] [55] Adam Paszke, Sam Gross, Francisco Massa, Adam Lerer, James Bradbury, Gregory Chanan, Trevor Killeen, Zeming Lin, Natalia Gimelshein, Luca Antiga, et al. 2019. PyTorch: An Imperative Style, High-Performance Deep Learning Library. In *Advances in Neural Information Processing Systems (NeurIPS)*, Vol. 32. 8024–8035.
- [1535] [56] Pratyush Patel, Esha Choukse, Chaojie Zhang, Aakanksha Shah, Íñigo Goiri, Saeed Maleki, and Ricardo Bianchini. 2024. Splitwise: Efficient Generative LLM Inference Using Phase Splitting. In *Proceedings of the 51st Annual International Symposium on Computer Architecture (ISCA)*. 118–132. <https://doi.org/10.1109/ISCA59077.2024.00019> Best Paper Award.
- [1536] [57] Hang Qi, Evan R. Sparks, and Ameet Talwalkar. 2017. Paleo: A Performance Model for Deep Neural Networks. In *Proceedings of the 5th International Conference on Learning Representations (ICLR)*. <https://openreview.net/forum?id=SyVVJ85lg>
- [1537] [58] Aurick Qiao, Sang Keun Agrawal, Anand Jayarajan, Moustafa Mittal, Amar Altaf, Michael Cho, and Gennady Pekhimenko. 2021. Pollux: Co-adaptive Cluster Scheduling for Goodput-Optimized Deep Learning. In *Proceedings of the 15th USENIX Symposium on Operating Systems Design and Implementation (OSDI)*. 1–18. Goodput estimation for co-optimizing resource allocation and training hyperparameters.
- [1538] [59] Jonathan Ragan-Kelley, Connelly Barnes, Andrew Adams, Sylvain Paris, Frédéric Durand, and Saman Amarasinghe. 2013. Halide: A Language and Compiler for Optimizing Parallelism, Locality, and Recomputation in Image Processing Pipelines. In *Proceedings of the 34th ACM SIGPLAN Conference on Programming Language Design and Implementation (PLDI)*. 519–530. <https://doi.org/10.1145/2491956.2462176> Pioneer separation of algorithm and schedule with learned cost models for autoscheduling.

1567
1568
1569
1570
1571
1572
1573
1574
1575
1576
1577
1578
1579
1580
1581
1582
1583
1584
1585
1586
1587
1588
1589
1590
1591
1592
1593
1594
1595
1596
1597
1598
1599
1600
1601
1602
1603
1604
1605
1606
1607
1608
1609
1610
1611
1612
1613
1614
1615
1616
1617
1618
1619
1620
1621
1622
1623

- 1625 [60] Samyam Rajbhandari, Jeff Rasley, Olatunji Rber, and Yuxiong He. 2020. ZeRO: 1626 Memory Optimizations Toward Training Trillion Parameter Models. In *Proceedings of the International Conference on High Performance Computing, Networking, 1627 Storage and Analysis (SC)*. 1–16. <https://doi.org/10.1109/SC41405.2020.00024>
- 1628 DeepSpeed ZeRO optimizer partitioning for memory-efficient distributed training.
- 1629 [61] Mehdi Rakhshanfar and Aliakbar Zarandi. 2021. A Survey on Machine Learning-based 1630 Design Space Exploration for Processor Architectures. *Journal of Systems Architecture* 121 (2021), 102339. <https://doi.org/10.1016/j.sysarc.2021.102339>
- 1631 [62] Saeed Rashidi, Srinivas Srinivasan, Kazem Hamedani, and Tushar Krishna. 2020. ASTRA-SIM: Enabling SW/HW Co-Design Exploration for Distributed 1632 DL Training Platforms. In *Proceedings of the IEEE International Symposium on Performance Analysis of Systems and Software (ISPASS)*. 81–92. <https://doi.org/10.1109/ISPASS48437.2020.00018>
- 1633 [63] Vijay Janapa Reddi et al. 2025. MLPerf Power: Benchmarking the Energy Efficiency 1634 of Machine Learning Inference. In *Proceedings of the IEEE International Symposium on High Performance Computer Architecture (HPCA)*. 1–14. Energy efficiency benchmarking for ML inference workloads.
- 1635 [64] Vijay Janapa Reddi, Christine Cheng, David Kanter, Peter Mattson, Guenther 1636 Schmuelling, Carole-Jean Wu, Brian Anderson, Maxim Breshekov, Mark Duber, et al. 2020. MLPerf Inference Benchmark. In *Proceedings of the 47th International 1637 Symposium on Computer Architecture (ISCA)*. 446–459. <https://doi.org/10.1109/ISCA45697.2020.00045> Standard ML inference benchmark suite with server and offline scenarios.
- 1638 [65] George F. Riley and Thomas R. Henderson. 2010. The ns-3 Network Simulator. 1639 *Modeling and Tools for Network Simulation* (2010), 15–34. https://doi.org/10.1007/978-3-642-12331-3_2
- 1640 [66] Arun F. Rodrigues, K. Scott Hemmert, Brian W. Barrett, Chad Kersey, Ron Oldfield, 1641 Marlo Weston, R. Risen, Jeanine Cook, Paul Rosenfeld, Elliott Cooper-Balis, and Bruce Jacob. 2012. The Structural Simulation Toolkit. In *ACM SIGMETRICS 1642 Performance Evaluation Review*, Vol. 38. 37–42. <https://doi.org/10.1145/1964218.1964225> Modular framework for system-level simulation, widely used for HPC and interconnect modeling.
- 1643 [67] Ananda Samajdar, Yuhao Zhu, Paul Whatmough, Matthew Mattina, and Tushar 1644 Krishna. 2019. A Systematic Methodology for Characterizing Scalability of DNN Accelerators using SCALE-Sim. In *Proceedings of the IEEE International 1645 Symposium on Performance Analysis of Systems and Software (ISPASS)*. 58–68. <https://doi.org/10.1109/ISPASS.2019.00016> Cycle-accurate systolic array simulator for DNN accelerator DSE.
- 1646 [68] Zhuomin Shen, Jaeho Kim, et al. 2025. AQUA: Network-Accelerated Memory 1647 Offloading for LLMs in Scale-Up GPU Domains. In *Proceedings of the 30th ACM 1648 International Conference on Architectural Support for Programming Languages and Operating Systems (ASPLOS)*. 1–16. <https://doi.org/10.1145/3676641.3715983> Improves LLM inference responsiveness by 20x through network-accelerated memory offloading.
- 1649 [69] Mohammad Shoeybi, Mostafa Patwary, Raul Puri, Patrick LeGresley, Jared Casper, 1650 and Bryan Catanzaro. 2020. Megatron-LM: Training Multi-Billion Parameter 1651 Language Models Using Model Parallelism. In *arXiv preprint arXiv:1909.08053*. 1652 Intra-layer tensor parallelism for large language model training.
- 1653 [70] Srinivas Sridharan, Taekyung Heo, Jinwoo Choi, Garyfallia Yu, Saeed Rashidi, William Won, Zhaodong Meng, and Tushar Krishna. 2023. Chakra: Advancing 1654 Performance Benchmarking and Co-design using Standardized Execution Traces. *arXiv preprint arXiv:2305.14516* (2023).
- 1655 [71] Foteini Strati, Zhendong Zhang, George Manos, Ixeia Sanchez Periz, Qinghao 1656 Hu, Tiancheng Chen, Berk Buzcu, Song Han, Pamela Delgado, and Ana Klimovic. 1657 2025. Sailor: Automating Distributed Training over Dynamic, Heterogeneous, and Geo-distributed Clusters. In *Proceedings of the 30th ACM Symposium on 1658 Operating Systems Principles (SOSP)*. 1–18. Automated distributed training with 1659 runtime/memory simulation over heterogeneous resources. ETH Zurich/MIT.
- 1660 [72] Ondrej Sykora, Alexis Rucker, Charith Mendis, Rajkishore Barik, Phitchaya Mangpo Phothilimthana, and Saman Amarasinghe. 2022. GRANITE: 1661 A Graph Neural Network Model for Basic Block Throughput Estimation. In *Proceedings of the IEEE International Symposium on Workload Characterization (ISWC)*. 1–13. <https://doi.org/10.1109/ISWC55918.2022.00014>
- 1662 [73] Vivienne Sze, Yu-Hsin Chen, Tien-Ju Yang, and Joel S. Emer. 2017. Efficient 1663 Processing of Deep Neural Networks: A Tutorial and Survey. In *Proceedings of the IEEE*, Vol. 105. 2295–2329. <https://doi.org/10.1109/JPROC.2017.2761740> Canonical DNN accelerator taxonomy covering dataflows, data reuse, and energy 1664 efficiency.
- 1665 [74] Philippe Tillet, H. T. Kung, and David Cox. 2019. Triton: An Intermediate 1666 Language and Compiler for Tiled Neural Network Computations. In *Proceedings of the 3rd ACM SIGPLAN International Workshop on Machine Learning and 1667 Programming Languages (MAPL)*. 10–19. <https://doi.org/10.1145/3315508.3329973> Tile-based GPU programming with heuristic performance model for kernel 1668 generation.
- 1669 [75] Adrian Tschand, Mohamed Awad, et al. 2025. SwizzlePerf: Hardware-Aware 1670 LLMs for GPU Kernel Performance Optimization. *arXiv preprint arXiv:2508.20258* 1671 (2025). LLM-based spatial optimization for GPU kernels, up to 2.06x speedup 1672 via swizzling.
- 1673 [76] Xizheng Wang, Qingxu Li, Yichi Xu, Gang Lu, Heyang Zhou, Sen Zhang, Yikai 1674 Zhu, Yang Liu, Pengcheng Zhang, Kun Qian, et al. 2025. SimAI: Unifying 1675 Architecture Design and Performance Tuning for Large-Scale LLM Training with 1676 Scalability and Precision. In *Proceedings of the 22nd USENIX Symposium on 1677 Networked Systems Design and Implementation (NSDI)*. 1–18. Full-stack LLM 1678 training simulator achieving 98.1% alignment with real-world results. Alibaba 1679 Cloud/Tsinghua.
- 1680 [77] Zixian Wang et al. 2025. SynPerf: Synthesizing High-Performance GPU Kernels 1681 via Pipeline Decomposition. *arXiv preprint* (2025). Under review.
- 1682 [78] Samuel Williams, Andrew Waterman, and David Patterson. 2009. Roofline: An 1683 Insightful Visual Performance Model for Multicore Architectures. *Commun. ACM* 52, 4 (2009), 65–76. <https://doi.org/10.1145/1498765.1498785>
- 1684 [79] William Won, Taekyung Heo, Saeed Rashidi, Saeed Talati, Srinivas Srinivasan, 1685 and Tushar Krishna. 2023. ASTRA-sim2.0: Modeling Hierarchical Networks and 1686 Disaggregated Systems for Large-Model Training at Scale. In *Proceedings of the 1687 IEEE International Symposium on Performance Analysis of Systems and Software (ISPASS)*. 283–294. <https://doi.org/10.1109/ISPASS57527.2023.00035>
- 1688 [80] Yannan Nelli Wu, Joel Emer, and Vivienne Sze. 2022. SparseLoop: An Analytical 1689 Approach to Sparse Tensor Accelerator Modeling. In *Proceedings of the 55th 1690 IEEE/ACM International Symposium on Microarchitecture (MICRO)*. 1–15. <https://doi.org/10.1109/MICRO56248.2022.00078>
- 1691 [81] Gyeong-In Yu, Jo Seong Jeong, Geon-Woo Kim, Soojeong Kim, and Byung-Gon 1692 Chun. 2022. ORCA: A Distributed Serving System for Transformer-Based 1693 Generative Models. In *Proceedings of the 16th USENIX Symposium on Operating 1694 Systems Design and Implementation (OSDI)*. 521–538.
- 1695 [82] Geoffrey X. Yu, Yubo Gao, Pavel Golber, and Asaf Cidon. 2021. Habitat: A 1696 Runtime-Based Computational Performance Predictor for Deep Neural Network 1697 Training. In *Proceedings of the USENIX Annual Technical Conference (ATC)*. 503– 1698 521.
- 1699 [83] Yi Zhai, Yu Cheng Wang, Peng Jiang, and Congming Kang. 2023. TLP: A Deep 1700 Learning-based Cost Model for Tensor Program Tuning. In *Proceedings of the 1701 28th ACM International Conference on Architectural Support for Programming 1702 Languages and Operating Systems (ASPLOS)*. 833–845. <https://doi.org/10.1145/3575693.3575736>
- 1702 [84] Li Lyra Zhang, Shihao Han, Jianyu Wei, Ningxin Zheng, Ting Cao, Yuqing Yang, 1703 and Yunxin Liu. 2021. nn-Meter: Towards Accurate Latency Prediction of Deep- 1704 Learning Model Inference on Diverse Edge Devices. In *Proceedings of the 19th 1705 Annual International Conference on Mobile Systems, Applications, and Services (MobiSys)*. 81–93. <https://doi.org/10.1145/3458864.3467882> Best Paper Award.
- 1706 [85] Lianmin Zheng, Chengfan Jia, Minmin Sun, Zhao Wu, Cody Hao Yu, Ameer Haj-Ali, Yida Wang, Jun Yang, Danyang Zhuo, Koushik Sen, Joseph E. Gonzalez, 1707 and Ion Stoica. 2020. Ansor: Generating High-Performance Tensor Programs 1708 for Deep Learning. In *Proceedings of the 14th USENIX Symposium on Operating 1709 Systems Design and Implementation (OSDI)*. 863–879.
- 1710 [86] Lianmin Zheng, Ruochen Liu, Junru Shao, Tianqi Chen, Joseph E. Gonzalez, 1711 Ion Stoica, and Zhihao Zhang. 2021. TenSet: A Large-scale Program Performance 1712 Dataset for Learned Tensor Compilers. In *Advances in Neural Information 1713 Processing Systems (NeurIPS)*, Vol. 34. 29876–29888.
- 1714 [87] Yinmin Zhong, Shengyu Liu, Junda Chen, Jianyu Hu, Yibo Zhu, Xuanzhe Liu, 1715 Xin Jin, and Hao Zhang. 2024. DistServe: Disaggregating Prefill and Decoding 1716 for Goodput-optimized Large Language Model Serving. In *Proceedings of the 18th 1717 USENIX Symposium on Operating Systems Design and Implementation (OSDI)*. 1718 1–18.
- 1719 [88] Vivienne Sze, Yu-Hsin Chen, Tien-Ju Yang, and Joel S. Emer. 2017. Efficient 1720 Processing of Deep Neural Networks: A Tutorial and Survey. In *Proceedings of the 1721 IEEE*, Vol. 105. 2295–2329. <https://doi.org/10.1109/JPROC.2017.2761740> Canonical DNN accelerator taxonomy covering dataflows, data reuse, and energy 1722 efficiency.
- 1723 [89] Philippe Tillet, H. T. Kung, and David Cox. 2019. Triton: An Intermediate 1724 Language and Compiler for Tiled Neural Network Computations. In *Proceedings of the 3rd ACM SIGPLAN International Workshop on Machine Learning and 1725 Programming Languages (MAPL)*. 10–19. <https://doi.org/10.1145/3315508.3329973> Tile-based GPU programming with heuristic performance model for kernel 1726 generation.
- 1727 [90] Adrian Tschand, Mohamed Awad, et al. 2025. SwizzlePerf: Hardware-Aware 1728 LLMs for GPU Kernel Performance Optimization. *arXiv preprint arXiv:2508.20258* 1729 (2025). LLM-based spatial optimization for GPU kernels, up to 2.06x speedup 1730 via swizzling.
- 1731 [91] Xizheng Wang, Qingxu Li, Yichi Xu, Gang Lu, Heyang Zhou, Sen Zhang, Yikai 1732 Zhu, Yang Liu, Pengcheng Zhang, Kun Qian, et al. 2025. SimAI: Unifying 1733 Architecture Design and Performance Tuning for Large-Scale LLM Training with 1734 Scalability and Precision. In *Proceedings of the 22nd USENIX Symposium on 1735 Networked Systems Design and Implementation (NSDI)*. 1–18. Full-stack LLM 1736 training simulator achieving 98.1% alignment with real-world results. Alibaba 1737 Cloud/Tsinghua.
- 1738 [92] Zixian Wang et al. 2025. SynPerf: Synthesizing High-Performance GPU Kernels 1739 via Pipeline Decomposition. *arXiv preprint* (2025). Under review.